TECHNICAL UNIVERSITY OF LIBEREC
Faculty of Mechanical Engineering

Heat transfer in horizontally oriented enclosure

Master Thesis

Study programme:	N2301 Mechanical Engineering
Study branch:	Machines and Equipment Design
Author:	**Dereje Yihun Amare**
Thesis Supervisors:	doc. Ing. Jaroslav Šulc, CSc.
	Department of Power Engineering Equipment

Liberec 2021

Master Thesis Assignment Form

Heat transfer in horizontally oriented enclosure

Name and surname: **Dereje Yihun Amare**
Identification number: S19000341
Study programme: N2301 Mechanical Engineering
Study branch: Machines and Equipment Design
Assigning department: Department of Power Engineering Equipment
Academic year: **2020/2021**

Rules for Elaboration:

Experimental determination of the angle dependency of the emissivity of horizontally oriented surfaces of the horizontally oriented air enclosures for surfaces that are 1) electrical conductors and 2) nonconductors. Experimentally determined values of the total heat flux through the enclosure will be compared with analytically determined values for enclosures modeled as an enclosures with reemitting vertical walls. All the measurements will be performed by means of the heat flow meter HFM/436/3/1 Lambda.

List of Specialised Literature:

1. Cengel, Y., Boles, M.A.: Heat and Mass Transfer (A Practical Approach)
2. Lienhard, J.H., Lienhard, J.H.: A Heat Transfer Textbook, Third ed., Philociston Press, Cambridge, Massachusetts
3. Ananthasayanan, G.: Heat Transfer in Horizontally Oriented Air Enclosure, Diploma Thesis, TUL Liberec, 2020

L.S.

prof. Dr. Ing. Petr Lenfeld   doc. Ing. Petra Dančová, Ph.D.
            Dean   Head of Department

Liberec   November 1, 2020

Declaration

I hereby certify, I, myself, have written my master thesis as an original and primary work using the literature listed below and consulting it with my thesis supervisor and my thesis counsellor.

I acknowledge that my bachelor master thesis is fully governed by Act No. 121/2000 Coll., the Copyright Act, in particular Article 60 – School Work.

I acknowledge that the Technical University of Liberec does not infringe my copyrights by using my master thesis for internal purposes of the Technical University of Liberec.

I am aware of my obligation to inform the Technical University of Liberec on having used or granted license to use the results of my master thesis; in such a case the Technical University of Liberec may require reimbursement of the costs incurred for creating the result up to their actual amount.

At the same time, I honestly declare that the text of the printed version of my master thesis is identical with the text of the electronic version uploaded into the IS/STAG.

I acknowledge that the Technical University of Liberec will make my master thesis public in accordance with paragraph 47b of Act No. 111/1998 Coll., on Higher Education Institutions and on Amendment to Other Acts (the Higher Education Act), as amended.

I am aware of the consequences which may under the Higher Education Act result from a breach of this declaration.

June 6, 2021   Dereje Yihun Amare

Acknowledgment

I would like to express my sincere gratitude to my supervisor, doc. Ing. Jaroslav Šulc, Csc., for the continuous support throughout the research work, for his patience, enthusiasm, motivation, and immense knowledge. His guidance helped me in all the time of writing this thesis. It was a great pleasure to work and discuss with him and a huge respect for his accountability.

I would like to sincerely thank the government of Czech Republic for giving me the opportunity to pursue my masters degree by granting me a scholarship for the entire duration of my study.

I would like to extend my deepest gratitude to the Department of Power Engineering Equipment, Faculty of mechanical engineering, of the Technical University of Liberec, Czech Republic, for admitting me and giving me the opportunity to do my master study on Machines and Equipment Design.

Furthermore, I also would like to thank the Ethiopian Institute of Agricultural Research /EIAR/ and Melkassa staff members for their constant support and encouragement.

My sincere thanks also goes to *ŠKODA AUTO* company for offering me an opportunity to be a part of the Simply Clever Hackathon competition event where I was exposed to innovative engineering technologies and selecting our group for the winning idea on predictive maintenance of timing belt project that enlighten and motivated me with the first glance of research.

Last and not least, my deepest appreciation goes to my family and friends for the encouragement and moral support to accomplish my work successfully.

Abstract

The presented diploma thesis deals with the heat transfer in rectangular, horizontally oriented air enclosures. The aim of this work was to determine the "effective emissivity" of horizontal surfaces delimiting air enclosures with vertical walls characterized as re-emitting. Enclosures with different heights of the air layer were created in the measuring space of the measuring device HFM/436/3/1E by means of square polystyrene boards with a nominal thickness of 0.01 m, in which a coaxial square hole with a side of 0.102 m was formed. The size of the hole coincided with the size of the aerial heat flow transducers of the measuring device. The horizontal surfaces delimiting the air enclosures were formed by three materials significantly differing in their electrical resistance, on which the angular distribution of photons emitted from the surface of these materials depends. The thermal conductivity of the enclosure determined by the measurement was compared with the thermal conductivity of the enclosure calculated for the gradually increasing emissivity of the horizontal surface of the enclosure in the range of emissivity forming the surroundings of the tabulated hemispherical emissivity. When equality between measured and calculated thermal conductivities was reached, the corresponding emissivity was designated as the effective emissivity of the horizontal surfaces for a given height of the air enclosure. This solution introduces an error into the value of effective emissivity caused by the fact that the angular dependence of emissivity of real horizontal surfaces was not taken into account.

Keywords

Heat Transfer, Conduction, Convection, Radiation, Air enclosure, Thermal conductivity, HFM/436/3/1E Lambda, Blackbody, Emissivity, View factor, Space resistance, Reradiating surface, Wavelength.

List of Symbols

A	surface area	m^2
E_{bi}	emissive power	W/m^2
EIT	effective value of emissivity	-
F	view factor	-
G_i	irradiation	W/m^2
i	trajectory	-
i, j	integers	-
I	radiant intensity	W/sr
J	radiosity	W/m^2
L	characteristic dimension	m
m	mass	kg
n	index of refraction of the medium	-
T	temperature	K
ΔT	temperature difference	K
$\dot{Q}$	heat flux	W
Q_i	net radiation heat transfer	W
QK	conductive component of the total heat flux through the air layer	W
QR	radiant component of the total heat flux through the air layer	W
QSC	radiant flux passing through the air layer calculated - re-emitting	W
QSE	radiant flux passing through the air layer calculated – Eqn. 30	W
QT	total heat flux through the assembly	W
R	thermal resistance of assembly	(m^2.K)/W
VM (I)	experimentally determined thermal conductivity of the air layer	W/(m^2.K)
VV (I,K)	calculated thermal conductivities	W/(m^2.K)
Z	thickness of air layer	m
ZS	thickness of the assembly	m

Greek symbols

α	absorptivity	-
$\alpha, \theta, \varphi, \phi$	angles	rad, °
ρ	density	kg/m^3
ε	emissivity	-
ε_θ	total directional emissivity	-
ε_λ	spectral hemispherical emissivity	-
ε (T)	total hemispherical emissivity	-
λ	wavelength	μm
k	thermal conductivity	W/(m.K)
Ω	solid angle	sr

Physical constants

c_0	the speed of light in vacuum	299792458 m/s
c_1	first radiation constant	$3.741771 \cdot 10^{-16}$ W.m^2
c_2	second radiation constant	$1.438777 \cdot 10^{-2}$ m.K
h	Planck's constant	$6.62607123 \cdot 10^{-34}$ J.s
k	Boltzmann's constant	$1.3806488 \cdot 10^{-23}$ J/K
σ	Stefan-Boltzmann constant	$5.670373 \cdot 10^{-8}$ W/(m^2.K^4)

Table of Contents

Table of Figures

List of Tables

11

CHAPTER - 1

1.1 INTRODUCTION

Heat transfer is a transfer of heat energy from one object to another. Heat can be transferred in three ways: by conduction, convection, and radiation. In this diploma thesis, experimental determination of the angle dependency of the emissivity of horizontally oriented surfaces in the horizontally oriented air enclosures for surfaces that are electrical conductors and nonconductors will be performed. Experimentally determined values of the total heat flux through the enclosure will be compared with analytically determined values for enclosures modeled as an enclosure with re-emitting vertical walls. This experiment is carried out on a measuring device HFM 436/3/1E Lambda. This instrument is used to measure the coefficient of thermal conductivity of solid insulating materials. The experimental setup is made and a series of measurements of heat flux will be taken to determine the angle dependency of the emissivity for aluminum foil, A4 paper surfaces on the top and bottom plate, and for the upper and lower plate of measuring instrument directly delimiting horizontally oriented surfaces of air enclosure. Calculations related to heat transfer mechanism will be carried out, and a comparison between measured and calculated values will be performed for all series of measurements.

CHAPTER - 2

2.1 HEAT TRANSFER

Heat transfer deals with the thermal energy transfer which may take place between material bodies as a result of a temperature difference. So, the temperature difference between the two objects is important to take place the heat transfer, no heat transfer can take place without temperature gradient. Heat transfer drives thermal energy from a higher temperature region to a lower temperature region. It seeks to explain how thermal energy may be transferred and how to predict the rate at which the energy exchange is accomplished under certain specified conditions. In contrast to reversible thermodynamics, which involves systems in equilibrium, the basic pre-requisite for heat transfer is a temperature difference, a system equilibrium, the basic pre-requisite for heat transfer is a temperature difference, a typical non-equilibrium feature. Reversible thermodynamic is able to predict the amount of energy required to change a system from one equilibrium state to another or to determine the final state as a result of energy interaction with the surroundings [1]. However, it cannot predict how fast the change will take place, and it does not consider the time and space evolution of a process.

In the beginning of the 19th century, scientists thought that all bodies contained an invisible fluid referred to as caloric. Caloric was classified into several properties, some of which proved to be inconsistent with nature. However, its most important feature was the flow of heat from hot to cold bodies. It was a very useful way scientist to think about heat. Then it had been superseded by the mid-19th century in favor of the mechanical theory of heat.

2.1.1 Modes of Heat Transfer

Heat can be transferred from one system to another in the form of energy. It can be transferred in three mechanisms;

- Conduction
- Convection
- Radiation

2.2 CONDUCTION

The physical foundation of conduction is the transfer of molecular motion to the neighboring molecules by collisions. The solid-body atoms situated in a crystalline substance (possibly also electrons in the case of metals) are vibrating about their equilibrium positions. If a part of the body surface is heated, e.g., an end of a rod by a flame, the adjacent atoms began to vibrate with larger and larger amplitudes. These, in turn, collide with their neighbors and transfer some of their energy in collisions. Slowly, atoms further down the rod increase their amplitude of vibration, and, in this manner, they transfer thermal energy, heat. Conduction heat transfer takes place mostly in solid-state substances. Conduction is also pronounced in fluids, provided that they are at rest or in a narrow layer close to a wall. If the fluid moves, the microscopic conduction process is usually overshadowed by a macroscopic motion involving heat convection [1].

The rate of the transfer of heat by conduction through a medium mainly depends on the geometry, thickness, material of the medium, and the temperature difference across the medium [2]. **Fourier's law** yields the microscopic description of conduction. Fourier's law gives the relationship between the temperature gradient and heat flow. It says that the heat flux that is ensuing from thermal conduction is proportional to the magnitude of the temperature gradient with opposite sign [3].

$$\dot{Q} = -k.A.\frac{dT}{dx} \tag{1}$$

Where, $\dot{Q}$ - Heat flux [W],

   k - Thermal conductivity [W/(m.K)],

   A - Surface area [m^2],

   $\frac{dT}{dx}$ - Temperature gradient [K/m].

From Eqn. 1, the heat transfer is directly proportional to the thermal conductivity of the material. The coefficient of thermal conductivity is an important factor for the rate of flow of heat. For different types of materials, the coefficient of thermal conductivity is different by the change in valence and crystal structure. Metals have high value and then go with liquid metals and gaseous, so on. For metals, the thermal conductivity increases with a decrease in temperature; for gases, the conductivity increases with an increase in temperature. In insulating materials, the conductivity increase with an increase in temperature. The thermal conductivity of the material is a measurement of the material's ability to conduct heat [4] [5]. A high value of thermal conductivity indicates that the material is a good thermal conductor, heat. On the contrary, a low value of of thermal conductivity indicates the material is a poor heat conductor or it's nonconductor/insulator [2]. It can be calculated as the rate of heat transfer through a unit thickness of the material per unit area and per unit of temperature difference [6].

2.3 CONVECTION

Convective heat transfer is a rather complex heat transfer mode. It combines the macroscopic flow of fluids and microscopic motion involving conduction. Namely, a macroscopic portion of the mass, also carrying thermal energy, is transported between two regions at different temperatures. As a rule, convection heat transfer occurs when heat is transferred between a solid surface and adjacent liquid or gas in motion. Also, It involves the combined effects of conduction and movement of fluid: the faster the fluid moves, the greater heat transfer by convection [1]. However, without the fluid motion, the heat transfer between a solid surface and the adjacent fluid is by pure conduction [7].

Suppose fluid motion is induced by a non-uniform distribution of temperature and density of fluid that is affected by gravity and buoyancy forces. In that case, the convection is referred to as free convection or natural convection [1].

2.3.1 Natural convection inside enclosures

Enclosures are frequently faced in practice, and heat transfer through it is of practical need. The heat transfer in enclosed spaces is complicated by the fact that the fluid in the enclosure is generally, it does not remain stationary. In a vertical enclosure, the fluid (liquid/gas) adjacent to the hotter surface rises and the fluid adjacent to the cooler one falls, setting off a rotational motion within the enclosure that enhances heat transfer through the enclosure.Typical examples of enclosures include wall cavities, solar collectors, and cryogenic chambers involving concentric cylinders or spheres [7]

Note that the characteristics of heat transfer through a horizontal enclosure depend on whether the hot plate is at the top or bottom, as shown in Fig. 1. **When the hot plate is at the top, no convection currents will develop in the enclosure since the lighter fluid will always be on top of the heavier fluid. In this case, heat transfer will be by pure conduction, and Nu = 1** [7][8].

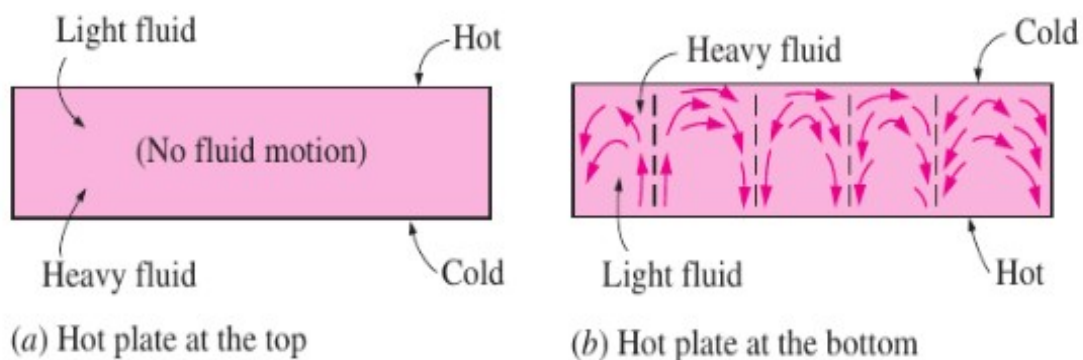Typical flow patterns in horizontal rectangular enclosures are shown below.

Figure 1: Convective currents in a horizontal enclosure with (a) hot plate at the top and (b) hot plate at the bottom [7].

2.4 THERMAL RADIATION

Each body emanates energy in the form of electromagnetic waves into its surroundings and to other bodies. This process is referred to as radiation. Also, at the same time, each body is irradiated by the other bodies and absorbs a portion of this energy. The rate of the mutual energy interaction by radiation strongly depends on temperature. Note that the only energy source on Earth is, in fact, the radiating Sun. The physical nature of this energy interaction takes the form of electromagnetic waves in the wavelength range $\lambda \in (8.10-7 - 8.10-4)$ m [1]. Contrarily to conduction and convection, heat transfer by radiation can also take place in a vacuum. Prior to radiation transfer, thermal energy is converted into the electromagnetic form, which propagates as waves. After incidence on a material body, the energy is converted back to thermal energy.

Thermal radiation is persistently emitted by all matter whose temperature is above absolute zero. It can be defined as the portion of the electromagnetic spectrum which extends from about 0.1 to 100 μm because the radiation emitted by bodies due to their temperature falls almost entirely within this wavelength range [7]. It has confirmed that useful to view electromagnetic radiation as the propagation of a set of discrete packets of energy is called **photons or quanta.** The energy of a photon or quanta is inversely proportional to its wavelength [9]. Therefore, shorter-wavelength radiation possesses larger photon energies [7].

2.4.1 Blackbody Radiation

A blackbody is an idealized body to serve as a model against that the radiative properties of real surfaces could also be compared. A blackbody is defined as an idealized physical body that is a perfect emitter and absorber of thermal radiation. At a specified temperature and wavelength, there is no surface that can emit more energy than a blackbody. It absorbs all incident radiation, regardless of wavelength and direction. In addition, a blackbody emits radiation energy uniformly in all directions per unit area normal to the direction of emission. A black body is a diffuse emitter —the term diffuse means that "independent of direction" [1].
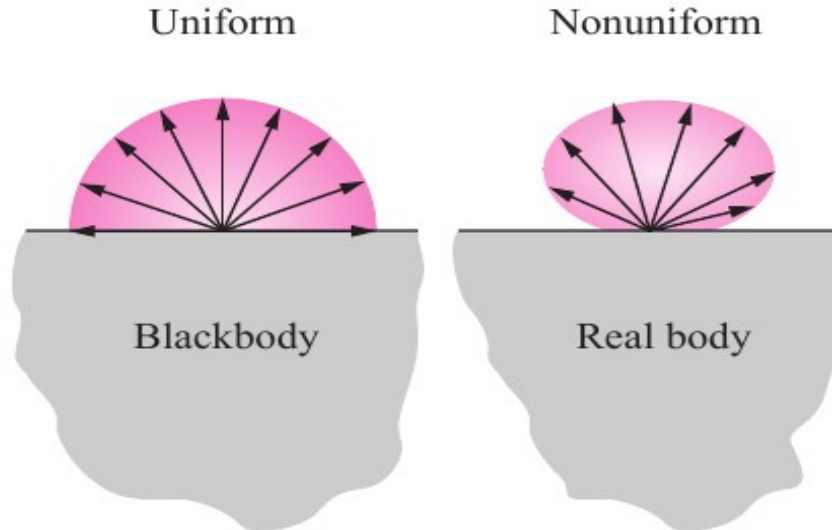
Figure 2: Direction of emission for real and blackbody [7].

The thermal radiation energy emitted by a blackbody per unit time and per unit surface area was determined through an experiment by Joseph Stefan in 1879 and expressed as

$$E_b(T) = \sigma T^4 \qquad [W/m^2] \tag{2}$$

where $\sigma = 5.67 * 10^{-8}$ W/(m^2.K^4) is the Stefan–Boltzmann constant and T is the absolute temperature of the surface in K.

The above relation was theoretically verified in 1884 by Ludwig Boltzmann. Eqn. (2) is known as the Stefan–Boltzmann law, and E_b is called the blackbody emissive power [1].

Note that the emission of thermal radiation is proportional to the fourth power of the absolute temperature.

The Stefan–Boltzmann law in Eqn. (2) gives the total blackbody emissive power E_b, that is the sum of the radiation emitted over all wavelengths. Sometimes we need to find the spectral blackbody emissive power, denoted by a symbol $E_{b\lambda}$, which is the amount of radiant energy emitted by an ideal blackbody at an absolute temperature T per unit time, per unit wavelength λ, and per unit surface area. It is given by Planck's law and expressed as [7][10].

$$E_{(b\lambda)}(\lambda,T) = \frac{C_1}{\lambda^5 \left[\exp\left(C_2/\lambda T\right) - 1 \right]} \qquad [W/(m^2.\mu m)] \tag{3}$$

where, $C_1 = 2\pi h c_o^2 = 3.742 *10^8$ (W.μ m^4)/m^2

$C_2 = hc_o/k = 1.439*10^4$ μ m.K

Also, T is the absolute temperature of the surface, λ is that the wavelength of the radiation emitted, and $k = 1.38065 * 10^{-23}$J/K is Boltzmann's constant. The relation here is valid for a surface in a very vacuum or a gas. For the other mediums, it has to be modified by substituting C_1 by C_1/n^2. Where, n is the that index of refraction of the medium. Noting that the term spectral indicates dependence on wavelength λ.

Planck's constant

Max Planck, in his theory, proposes a package of discrete energy is called photons. proportional to its wavelength [3][11].

$$E = hc/\lambda \tag{4}$$

Where, $h = 6.6256*10-34$ J.s is Planck's constant.
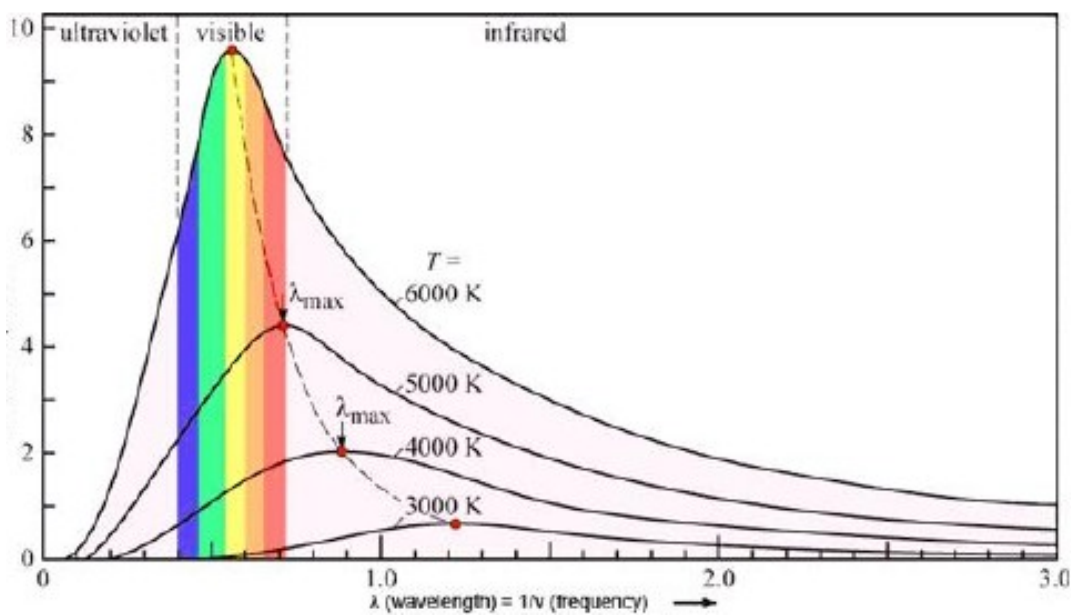
Figure 3: The variation of emissive power of blackbody with wavelength for several temperatures [3][6].

From Fig. 3, we can observe that [3], [12]

- The wavelength is a continuous function of emitted radiation. The temperature at any specific point increases the wavelength and reaches a peak, and then temperature decreases with an increase in wavelength.
- Radiation emitted at any wavelength increases with an increase in temperature.
- As the temperature increase, the curve shift to the left to a shorter wavelength region.
- The sun emits radiation, and it is considered as a blackbody at 5780 K and in the visible spectrum region when it reaches its peak.

Wien's displacement law

States that the wavelength of peak radiance and peak exitance is inversely proportional to the temperature T (in Kelvin). It gives the specific temperature at which the peak wavelength occurs. (λT) max power = 2897.8 μm.K
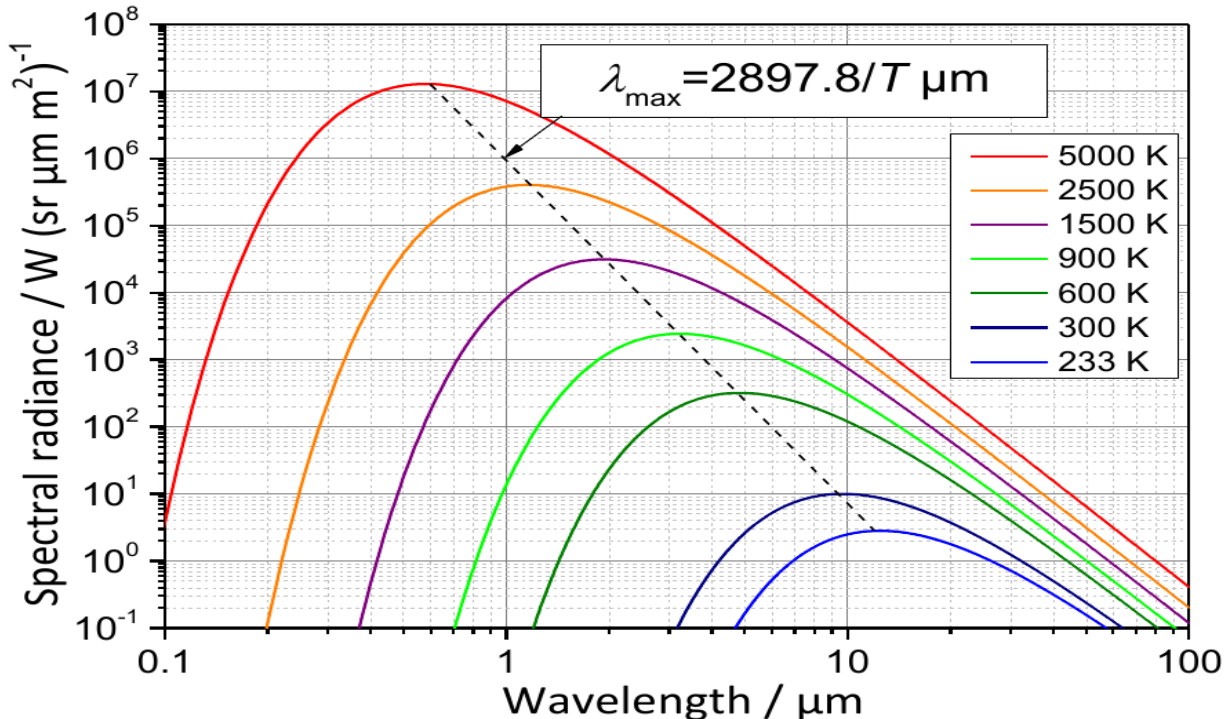
Figure 4: The spectral radiance of a blackbody according to Planck's law plotted for various temperatures ranging from 233 K to 5000 K [13].

The peak of the solar radiation, for instance, occurs at $\lambda = 2897.8/5780 = 0.50$ μm, which is close to the middle of the visible range. The peak of the emitted radiation by a surface at room temperature (T = 298 K) occurs at a wavelength of 9.72 μm, which is well into the infrared region of the spectrum.

2.4.2 Emissivity

Emissivity explains the relative ability of a material's surface to emit radiation energy. The emissivity of a surface is defined as the ratio of radiance emitted by the material surface at a given temperature to the radiance of a blackbody at the same temperature T. It is a dimensionless quantity, denoted by ε, and varies between zero and one ($0 \leq \varepsilon \leq 1$) [13][14]. Emissivity measures how close a surface is to a black body, for which $\varepsilon = 1$. The emissivity of a real surface is not a constant. On the contrary, it varies with the temperature of the surface as well as the wavelength and direction of the emitted radiation. Thus, different emissivities can be defined for a surface, depending on the effects considered. The most basic emissivity of a surface at a specified temperature T is the spectral directional emissivity, which is the ratio of the intensity of radiance emitted by the surface at a

given wavelength in a given direction to the intensity of the radiance emitted by a blackbody at the same temperature T at the same wavelength [7]

That is,
$$E_{(\lambda\theta)}(\lambda,\theta,\phi,T) = \frac{I_{(\lambda,e)}(\lambda,\theta,\phi,T)}{I_{(b\lambda)}(\lambda,T)}$$
(5)

Where the subscript λ is used to represents spectral, and θ is directional quantities, note that radiation intensity for a blackbody is independent of direction. Thus it has no functional dependence on θ and ϕ [7][12].

The total directional emissivity is defined as in a like manner by using total intensities (intensities integrated over all wavelengths) as:
$$\varepsilon_\theta(\theta,\varphi,T) = \frac{I_e(\theta,\varphi,T)}{I_b(T)}$$
(6)

Note that the integral of the rate of radiation energy emitted at a given wavelength per unit surface area over the whole hemisphere is spectral emissive power; It can be formulated as [7][15]:
$$\varepsilon_\lambda(\lambda,T) = \frac{E_\lambda(\lambda,T)}{E_{(b\lambda)}(\lambda,T)}$$
(7)

Finally, the total hemispherical emissivity, defined in terms of the radiation energy emitted over all wavelengths in all directions as [7] :
$$\varepsilon(T) = \frac{E(T)}{E_b(T)}$$
(8)

Therefore, the total hemispherical emissivity (or simply the "average emissivity") of a surface at a given temperature represents the ratio of the total radiance energy emitted by the surface to the radiance energy emitted by an ideal blackbody of the same surface area, and temperature.

Tab. 1 lists the emissivity ε and the solar absorptivity α_s of the surfaces of some common materials. Surfaces that are intended to collect solar energy, such as the absorber surfaces of solar collectors, are desired to have high α_s but low ε values to maximize the absorption of solar radiation and to minimize the emission of radiation [7].

Table 1: Comparison of the solar absorptivity α_s of some surfaces with their emissivity ε at room temperature [7].

Surface	α_s	ε
Aluminum		
Polished	0.09	0.03
Anodized	0.14	0.84
Foil	0.15	0.05
Copper		
Polished	0.18	0.03
Tarnished	0.65	0.75
Stainless steel		
Polished	0.37	0.60
Dull	0.50	0.21
Plated metals		
Black nickel oxide	0.92	0.08
Black chrome	0.87	0.09
Concrete	0.60	0.88
White marble	0.46	0.95
Red brick	0.63	0.93
Asphalt	0.90	0.90
Black paint	0.97	0.97
White paint	0.14	0.93
Snow	0.28	0.97
Human skin		
(caucasian)	0.62	0.97

Tab. 2 lists typical values of the total emittance for a variety of substances. Notice that most metals have quite low emittances, unless they are not oxidized. Most nonmetals have emittances that are pretty high, approaching the blackbody limit of the unit.

Table 2: Total emittances for a variety surfaces [3].

Metals			Nonmetals		
Surface	Temp. (°C)	ε	Surface	Temp. (°C)	ε
Aluminum			Asbestos	40	0.93–0.97
Polished, 98% pure	200–600	0.04–0.06	Brick		
Commercial sheet	90	0.09	Red, rough	40	0.93
Heavily oxidized	90–540	0.20–0.33	Silica	980	0.80–0.85
Brass			Fireclay	980	0.75
Highly polished	260	0.03	Ordinary refractory	1090	0.59
Dull plate	40–260	0.22	Magnesite refractory	980	0.38
Oxidized	40–260	0.46–0.56	White refractory	1090	0.29
Copper			Carbon		
Highly polished electrolytic	90	0.02	Filament	1040–1430	0.53
Slightly polished to dull	40	0.12–0.15	Lampsoot	40	0.95
Black oxidized	40	0.76	Concrete, rough	40	0.94
Gold: pure, polished	90–600	0.02–0.035	Glass		
Iron and steel			Smooth	40	0.94
Mild steel, polished	150–480	0.14–0.32	Quartz glass (2 mm)	260–540	0.96–0.66
Steel, polished	40–260	0.07–0.10	Pyrex	260–540	0.94–0.74
Sheet steel, rolled	40	0.66	Gypsum	40	0.80–0.90
Sheet steel, strong rough oxide	40	0.80	Ice	0	0.97–0.98
Cast iron, oxidized	40–260	0.57–0.66	Limestone	400–260	0.95–0.83
Iron, rusted	40	0.61–0.85	Marble	40	0.93–0.95
Wrought iron, smooth	40	0.35	Mica	40	0.75
Wrought iron, dull oxidized	20–360	0.94	Paints		
Stainless, polished	40	0.07–0.17	Black gloss	40	0.90
Stainless, after repeated heating	230–900	0.50–0.70	White paint	40	0.89–0.97
			Lacquer	40	0.80–0.95
Lead			Various oil paints	40	0.92–0.96
Polished	40–260	0.05–0.08	Red lead	90	0.93
Oxidized	40–200	0.63	Paper		
Mercury: pure, clean	40–90	0.10–0.12	White	40	0.95–0.98
Platinum			Other colors	40	0.92–0.94
Pure, polished plate	200–590	0.05–0.10	Roofing	40	0.91
Oxidized at 590°C	260–590	0.07–0.11	Plaster, rough lime	40–260	0.92
Drawn wire and strips	40–1370	0.04–0.19	Quartz	100–1000	0.89–0.58
Silver	200	0.01–0.04	Rubber	40	0.86–0.94
Tin	40–90	0.05	Snow	10–20	0.82
Tungsten			Water, thickness ≥0.1 mm	40	0.96
Filament	540–1090	0.11–0.16	Wood	40	0.80–0.90
Filament	2760	0.39	Oak, planed	20	0.90

2.4.3 The View Factor

Heat transfer by radiation between surfaces depends on the orientation of the surfaces relative to each other, their radiation properties and temperatures. The view factor is the effect of orientation on heat transfer by radiation between two surfaces, a purely geometric quantity, and is an independent of surface properties and temperature. It's also called shape factor, configuration factor, or angle factor. The view factor is based on the assumption that the surfaces are diffuse emitters and diffuse reflectors are called **the diffuse view factor [7] [16]**.

The view factor from a surface i to a surface j is denoted by $F_{i \to j}$ or just F_{ij}, and is defined as

F_{ij} = the fraction of the radiation leaving surface i that strikes surface j directly

$F_{i \to j}$ or F_{ij} emphasizes that the view factor is for radiation that travels from surface i to surface j.

The total rate at which radiation leaves the entire A1(via emission and re-flection) in all directions is

$$Q_{A1} = J_1 A_1 = \pi I_1 A_1 \tag{9}$$

Dividing this by the total radiation leaving A_1 (from Eqn. (9) gives the fraction of radiation leaving A_1 that strikes A_2, which is the view factor $F_{A1 \to A2}$ (or F_{12} for short).

$$F_{12} = F_{(A1 \to A2)} = \frac{Q_{(A1 \to A2)}}{Q_{(A1)}} = \frac{1}{A_1} \int_{A2} \int_{A1} \frac{\cos\theta_1 \cos\theta_2}{\Pi r^2} dA_1 dA_2 \tag{10}$$

The view factor $F_{A1 \to A2}$ is readily determined from Eqn. (10) by interchanging the subscripts 1 and 2.

$$F_{21} = F_{(A2 \to A1)} = \frac{Q_{(A2 \to A1)}}{Q_{(A2)}} = \frac{1}{A_2} \int_{A2} \int_{A1} \frac{\cos\theta_1 \cos\theta_2}{\Pi r^2} dA_1 dA_2 \tag{11}$$
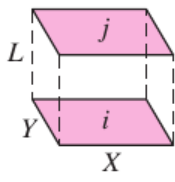
Noting that I_1 is constant, but r, θ_1, and θ_2 are variables. Also, the integrations can be performed in any order since the integration limits are constants. These relations confirm that the view factor between two surfaces depends on their relative orientation and distance between them.

Combining Eqns. (10) and (11) after multiplying the former by A_1 and the latter by A_2, gives [7]

$$A_1 F_{12} = A2 F_{21} \tag{12}$$

This is called the reciprocity relation for view factors; it allows the calculation of a view factor. The view factors for hundreds of common geometries are evaluated in several publications, and the results are given in the analytical, graphical, and tabular form. View factors for aligned parallel rectangles geometry (3D) are presented in Tab. 3.

Table 3 view factor expressions for aligned parallel rectangles geometry of finite size 3D [7][3][13].

Geometry	Relation
Aligned parallel rectangles	$\overline{X} = X/L$ and $\overline{Y} = Y/L$ $$F_{i \to j} = \frac{2}{\pi \overline{X}\overline{Y}} \left\{ \ln\left[\frac{(1+\overline{X}^2)(1+\overline{Y}^2)}{1+\overline{X}^2+\overline{Y}^2} \right]^{1/2} \right.$$ $$+ \overline{X}(1+\overline{Y}^2)^{1/2} \tan^{-1} \frac{\overline{X}}{(1+\overline{Y}^2)^{1/2}}$$ $$+ \overline{Y}(1+\overline{X}^2)^{1/2} \tan^{-1} \frac{\overline{Y}}{(1+\overline{X}^2)^{1/2}}$$ $$\left. - \overline{X}\tan^{-1}\overline{X} - \overline{Y}\tan^{-1}\overline{Y} \right\}$$

According to this relation, FHH followed by this formula, (13)

$$FHH = \frac{2}{\Pi \overline{X}\ \overline{Y}} \left\{ \ln\left[\frac{(1+\overline{X}^2)(1+\overline{Y}^2)}{1+\overline{X}^2+\overline{Y}^2} \right]^{\frac{1}{2}} + \overline{X}\ (1+\overline{Y}^2)^{\frac{1}{2}} \tan^{-1} \frac{\overline{X}}{(1+\overline{Y}^2)^{\frac{1}{2}}} \right\}$$

$$\left\{ + \overline{Y}\ (1+\overline{X}^2)^{\frac{1}{2}} \tan^{-1} \frac{\overline{Y}}{(1+\overline{X}^2)^{\frac{1}{2}}} - \overline{X}\ \tan^{-1}\overline{X}\ - \overline{Y}\ \tan^{-1}\overline{Y}\ \right\}$$

Where, $\overline{X} = X/L$ and $\overline{Y} = Y/L$

The conservation of energy principle requires the entire radiation leaving any surface i of an enclosure to be intercepted by the surfaces of an enclosure. Therefore, the sum of view factors from surface i of an enclosure to all surfaces of an enclosure, including to itself, must equal one or unity. This is called the **summation rule** for an enclosure [7].

$$\sum_{j=1}^{N} \left(F_{(i \to j)} \right) = 1 \tag{14}$$

where N - is the number of surfaces of enclosure. For instance, applying the summation rule to surface 1 of a three-surface enclosure yields.

$$\sum_{j=1}^{N} \left(F_{(i \to j)} \right) = F_{(1 \to 1)} + F_{(1 \to 2)} + F_{(1 \to 3)} = 1 \tag{15}$$

The summation rule can also be applied to each surface of an enclosure by varying the index i from 1 to N. Hence, the summation rule applied to each of the N surfaces of enclosures gives N relations for the determination of a certain view factors.

Note that, for plane surface $F_{1 \to 1} = 0$ so, from the above releation $FHC + FHH = 1.0$ we can calculate FHC as follows $\quad FHC = 1.0 - FHH \tag{16}$

2.4.4 Radiation heat transfer: diffuse, gray surfaces

The analysis of heat transfer by radiation in enclosures consisting of black surfaces is relatively easy, but most enclosures encountered in a real scenario involves nonblack surfaces, which allow multiple reflections to occur. The radiation analysis of such enclosures becomes very complicated unless some simplifying assumptions are made [7].

To make a simple possible radiation analysis, it is normal to assume the surfaces of an enclosure to be opaque, diffuse, and gray. In other words, the surfaces are nontransparent, diffuse emitters and diffuse reflectors, and their radiation properties are independent of wavelength.
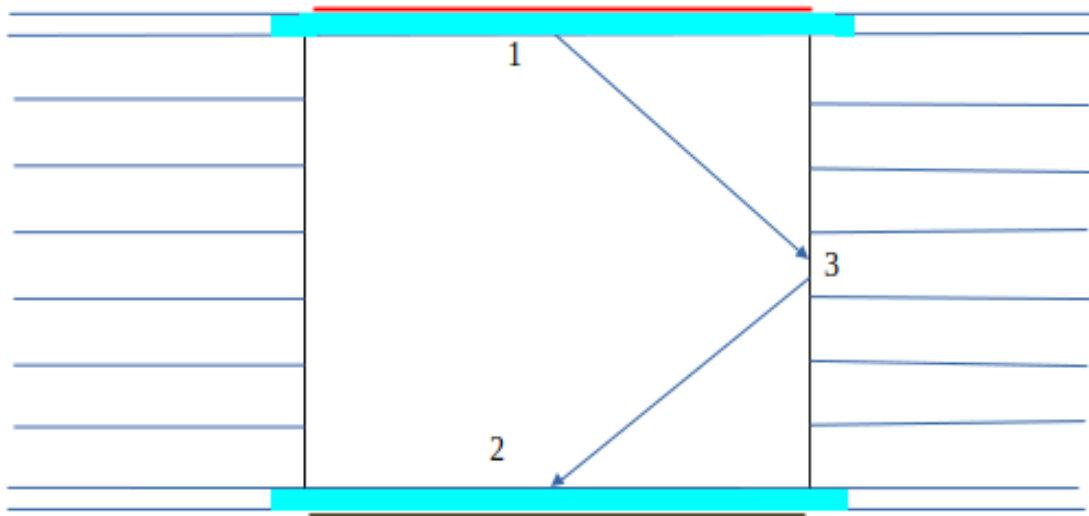
Figure 5: Schematic representation of experimental arrangement [own].

Where, 1- surface with higher temperature, 2- surface with lower tempreature, and 3- surface of vertical wall with decreasing temperature from surface 1 to 2.

Radiosity

A surface emits radiation and reflects it too, hence the radiation leaving a surface consists of emitted and reflected parts. The calculation of radiation between surfaces involves the total radiant energy expelled from a surface, with no respect to its origin. The total heat energy by radiation leaving a surface per unit time and per unit area is the radiosity and is denoted by letter J [7].

For a surface i, that is gray and opaque ($\varepsilon_i = \alpha_i$ and $\alpha_i + \rho_i = 1$), the radiosity can be expressed as

$$J_i = \text{(Radiation emitted by surface } i) + \text{(Radiation reflected by surface } i)$$

$$= \varepsilon_i E_{bi} + \rho G_i$$

$$= \varepsilon_i E_{bi} + (1 - \varepsilon_i) G_i \qquad [\text{W/m}^2] \qquad (17)$$

where $E_{bi} = \sigma T_i^4$ is the blackbody emissive power of surface i and G_i is irradiation (i.e., the radiant energy incident on surface i per unit time per unit area).

For a surface that can be approximated as a blackbody ($\varepsilon_i = 1$), the radiosity is formulated as

$$J_i = E_{bi} = \sigma T_i^4 \qquad \text{(blackbody)} \tag{18}$$

This implicates, the radiosity of a blackbody is equal to its emissive power. This happens, as a blackbody surface does not reflect any radiation, and thus radiation coming from a blackbody is only due to emission. [7].
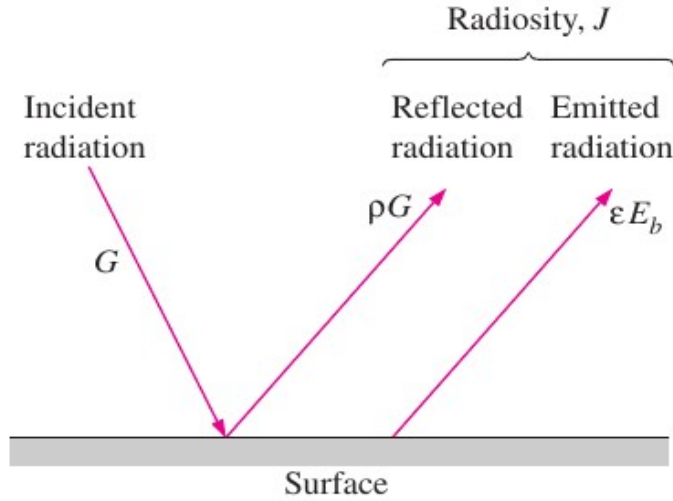

Figure 6: Radiosity represents the sum of the radiation energy emitted and reflected by a surface [7].

2.4.5 Net Radiation Heat Transfer to or from a Surface

The net rate of radiation energy from a surface i of surface area A_i is denoted by Q_i and is expressed as

Q_i = (Radiation leaving entire surface i) - (Radiation incident on entire surface i)

$$= A_i (J_i - G_i) \qquad \text{[W]} \tag{19}$$

Solving for G_i from Eqn. (17) and substituting into Eqn. (19) yields

$$Q_i = A_i \left(J_i - \varepsilon_i E_{bi}/1 - \varepsilon_i \right) = A_i E_i/1 - \varepsilon_i \left(E_{bi} - J_i \right) \quad \text{[W]} \tag{20}$$

In an electrical analogy to Ohm's law, the equation can be rearranged as

$$Q_i = \left(E_{bi} - J_i \right)/R_i \tag{21}$$

$$\text{where,} \quad R_i = \frac{1 - \varepsilon_i}{A_i \varepsilon_i} \tag{22}$$

R_i is the surface resistance. The quantity (E_{bi} - J_i) corresponds to a potential difference and the net rate of radiation heat transfer corresponds to current in the electrical analogy.

The direction of the net heat transfer by radiation depends on the relative magnitudes of J_i (radiosity) and E_{bi} (emissive power of a blackbody at the surface temperature). The radiation will be directed from the surface if ($E_{bi} > J_i$) and towards the surface if ($J_i > E_{bi}$).

A negative value for Q_i indicates that heat is transferred to the surface. All this radiation energy gained must be dissipated from the other side of the surface through some transfer mechanism if the surface temperature is to remain constant [7].

The surface resistance for a blackbody is zero since $\varepsilon_i = 1$ and $J_i = E_{bi}$. The net rate of radiation heat transfer in this case is determined directly from Eqn. (19).

Some surfaces encountered in numerous applications of heat transfer are modeled as being adiabatic since their backsides are well insulated and the net transfer of heat through them is zero. When the convective effects on the front (heat transfer) side of such a surface is negligible and steady state conditions are reached, the surface must lose as much radiant energy as it gains, and thus $Q_i = 0$. In such situations, the surface is said to reradiate all the radiation energy it receives, and such a surface is called a reradiating surface. Setting $Q_i = 0$ in Eqn. 21 yields [7]

$$J_i = E_{bi} = \sigma T_i^4 \qquad [\text{W/m}^2] \qquad (23)$$

Hence, the temperature of a reradiating surface under steady conditions can be easily determined from the equation mentioned above when its radiosity is known. Note that the reradiating surface temperature is independent of its emissivity.

In the analysis of radiation, the surface resistance of a reradiating surface is is not taken into consideration as there is no net heat transfer through it.

2.4.6 Net Radiation Heat Transfer between Any Two Surfaces

Realizing that the radiosity J represents the rate of radiation leaving from a surface per unit area and the view factor $F_{i \to j}$ represents the fraction of radiation leaving from surface i that strikes surface j, the net rate of radiation heat transfer from surface i to surface j can be shown as [7]

$Q_{i \to j} = ($ Radiation leaving the entire surface i that the strikes surface $j) -$

$\qquad$ (Radiation leaving the entire surface j that the strikes surface $i)$

$$\qquad = A_i J_i F_{i \to j} - A_j J_j F_{j \to i} \qquad [\text{W}] \qquad (24)$$

Applying the reciprocity relation $A_i F_{i \to j} = A_j F_{j \to i}$ yields

$$Q_{i \to j} = A_i F_{i \to j} \; (J_i - J_j) \qquad [\text{W}] \qquad (25)$$

In analogy to Ohm's law, the equation can be rearanged as

$$Q_{i \to j} = \left(J_i - J_j \right) / R_{i \to j} \qquad [\text{W}] \qquad (26)$$

where $\quad R_{(i \to j)} = 1 / A_i F_{(i \to j)} \qquad (27)$

The direction of the net heat transfer by radiation between two surfaces depends on the relative magnitudes of J_i and J_j. A positive value for $Q_{i \rightarrow j}$ indicates that net heat transfer is from surface i to surface j. A negative value indicates that the opposite.

In an N-surface enclosure, the principle of conservation energy requires the net heat transfer from surface i be equal to the sum of the net transfer of heat from surface *i* to each of the N surfaces of the enclosure [7].

Note that $Q_{i \rightarrow j}$ (the net rate of heat transfer from a surface to itself) is zero regardless of the shape of the surface. Combining Eqs. 10 and 15 gives

$$Q_{net\,i} = \frac{\varepsilon_{bi} - J_i}{\dfrac{1 - \varepsilon_i}{\varepsilon_i A_i}} = \sum_j \left(\frac{J_i - J_j}{1 / A_i F_{i \rightarrow j}} \right) \tag{28}$$

In a situation with three surfaces as shown in Fig. 7, leads to three equations [3][1].

$$Q_{net\,1}, \text{ at node } J_1 : \quad \frac{\varepsilon_{b1} - J_1}{\dfrac{1 - \varepsilon_1}{\varepsilon_1 A_1}} = \frac{J_1 - J_2}{\dfrac{1}{A_1 F_{(1 \rightarrow 2)}}} + \frac{J_1 - J_3}{\dfrac{1}{A_1 F_{(1 \rightarrow 3)}}} \tag{29 a}$$

$$Q_{net\,2}, \text{ at node } J_2 : \quad \frac{\varepsilon_{b2} - J_2}{\dfrac{1 - \varepsilon_2}{\varepsilon_2 A_2}} = \frac{J_2 - J_1}{\dfrac{1}{A_1 F_{(1 \rightarrow 2)}}} + \frac{J_2 - J_3}{\dfrac{1}{A_2 F_{(2 \rightarrow 3)}}} \tag{29 b}$$

$$Q_{net\,3}, \text{ at node } J_3 : \quad \frac{\varepsilon_{b3} - J_3}{\dfrac{1 - \varepsilon_3}{\varepsilon_3 A_3}} = \frac{J_3 - J_1}{\dfrac{1}{A_1 F_{(1 \rightarrow 3)}}} + \frac{J_3 - J_2}{\dfrac{1}{A_2 F_{(2 \rightarrow 3)}}} \tag{29 c}$$

If the temperatures T1, T2, and T3 are known (so that ε_{b1}, ε_{b2}, ε_{b3} are known), these equations can be solved simultaneously for the three unknowns, J_1, J_2, and J_3. After they are solved, one can compute the net heat transfer to or from any body (*i*) from either of Eqn. (28).
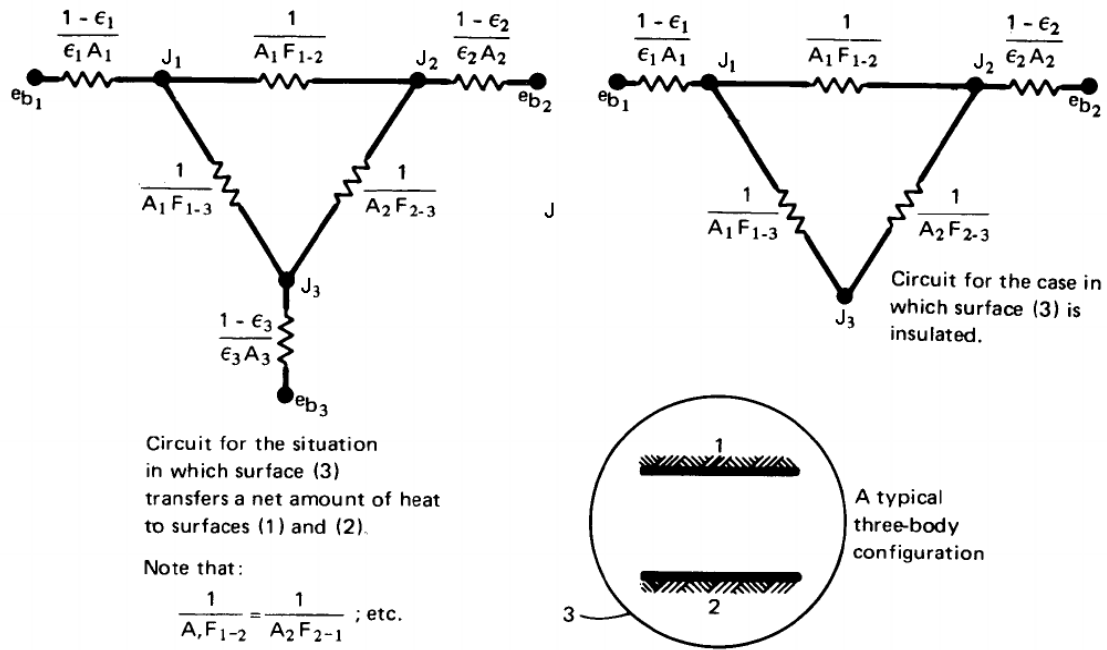
Figure 7: The electrical circuit analogy for radiation among three gray surfaces [3].

An insulated wall. If a wall is adiabatic, $Q_{net} = 0$ at that wall. For example, if wall (3) is insulated, then Eqn. (28) shows that $\varepsilon_{b3} = J_3$. We can eliminate one leg of the circuit, as shown on the right-hand side of Fig. 7; likewise, the left-hand side of Eqn. (29 c) equals zero. **This means that all radiation absorbed by an adiabatic wall is immediately reemitted. Such walls are sometimes called "reemitting" or "refractory surfaces" in discussing thermal radiation [3].**

The circuit for an insulated wall can be treated as a series-parallel circuit, since all the heat from body (1) flows to body (2), even if it does so by travelling first to body (3) [3].

Then

$$Q_{net\ 1} = \frac{\varepsilon_{b1} - \varepsilon_{b2}}{\dfrac{1-\varepsilon_1}{\varepsilon_1 A_1} + \dfrac{1}{\dfrac{1}{1/(A_1 F_{(1\rightarrow3)}) + 1/(A_2 F_{(2\rightarrow3)})} + \dfrac{1}{1/A_1 F_{(1\rightarrow2)}}} + \dfrac{1-\varepsilon_2}{\varepsilon_2 A_2}}$$

If the surface area and emissivity are the same so the above formula is simplified as follows,

$$Q_{net\ 1} = \frac{\varepsilon_{b1} - \varepsilon_{b2}}{\dfrac{2*(1-\varepsilon)}{\varepsilon*A} + \dfrac{1}{\dfrac{1}{\dfrac{2}{(A*FHC(I))}} + \dfrac{1}{\dfrac{1}{(A*FHH)}}}} \tag{30}$$

From this equation follows that heat transfer by radiation is independent of temperature and emissivity of the vertical walls of enclosure.

28

2.5 PHYSICAL PROPERTIES OF MATERIALS

To calculate the total heat flux and temperature gradient of a material, we have to know the coefficient of thermal conductivity and emissivity of the material we used for this study; air, aluminum foil, and paper.

2.5.1 Properties of air

Thermal conductivity of air is 0.024074 W/(m·K) [17], 0.02514 W/(m·K) [7] and 0.024 W/(m·K) [7].

at 0 °C, 20 °C and 25 °C respectively. Experimentally determined co-efficient of thermal conductivity of air at 20 °C, Cl = 0.0231 W/(m·K) [6].

2.5.2 Properties of aluminum foil

Thermal conductivity of aluminum foil is 250 W/(m·K) [7]. The density of aluminum foil is 2.7 g/cm³. The emissivity of aluminum for highly polished, commercial sheet, heavily oxidized and surface roofing is 0..39-0.057, 0.09, 0.20-0.30 and 0.216, respectively [18]. The emissivity of aluminum foil is shown in Tab. 4.

Table 4: Emissivity of aluminum foil with wavelength [19].

Material	Wavelength (µm)	Emissivity
Aluminum: foil	3	0.09
Aluminum: foil	10	0.04

2.5.2 Properties of paper

Thermal conductivity of paper is 0.05 W/(m·K) [20]. The emissivity of paper is shown in Tab. 5.

Table 5: Emissivity of paper with wavelength [19].

Material	Wavelength (µm)	Emissivity
paper: white	2-5.6	0.68
paper: white bond	8-14	0.90

CHAPTER - 3

3.1 MATERIALS AND METHODS

The HFM 436/3/1E Lambda measuring device was used for the experimental study of the heat transfer process in a rectangular horizontally oriented air enclosure. This device is designed for measuring the coefficients of thermal conductivity of insulating materials. The arrangement of the basic components of the measuring device is shown in Fig. 8.
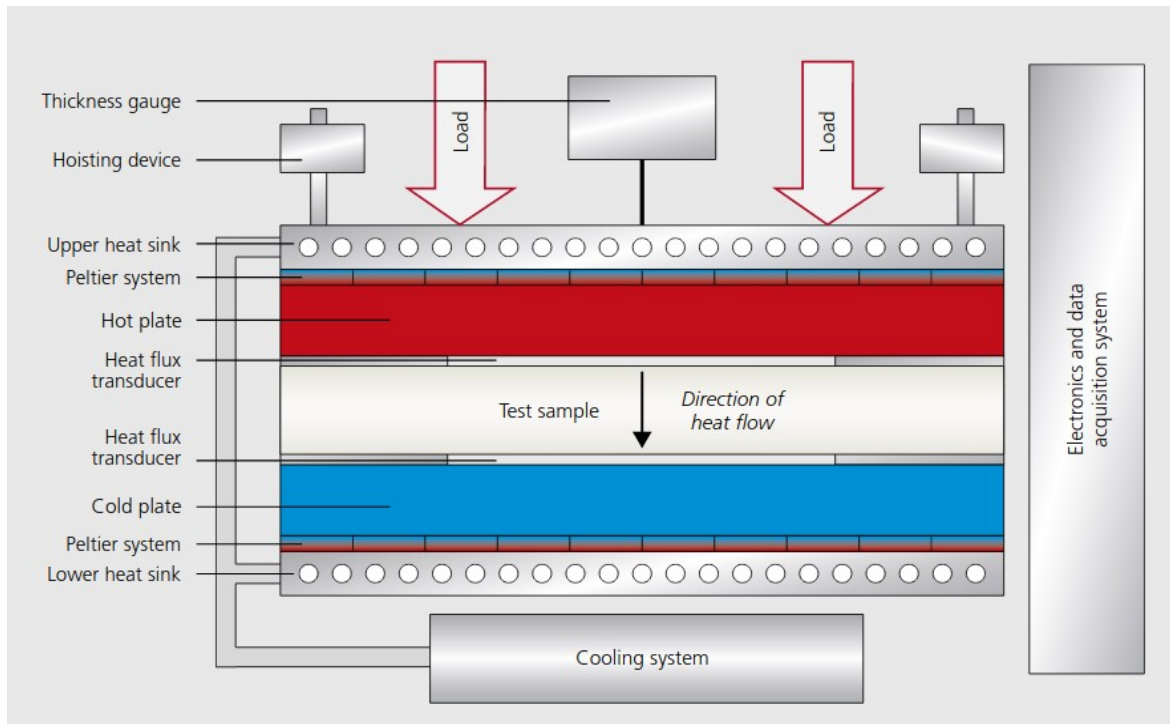

Figure 8: Components of measuring device [23]

This device belongs to the category of measuring devices based on the so-called "steady-state" relative measuring method. The determination of the coefficient of thermal conductivity of the material is based on determining of the heat flow through the measured material using calibrated planar heat flux transducers coaxially built into the hot and cold plate of the measuring device. By means of heat flux through the sample, the temperature difference across the sample and thickness of the sample, after reaching preselected thermal equilibrium state, heat conductivity and thermal resistance of the sample are determined.

The general working principle usually comprises of a material sample with thickness L, kept between two plates. The temperature of the plates can be set by the user. The temperature of the plates is controlled by the Peltier system, which is done using an integral fluid circle. This fluid is then cooled by an external chiller. The thermocouple is used to measure the temperature drop across the material.

Heat flux transducers are mounted on each plate. These transducers measure the plate's voltage proportional to the flow of heat. Heat flux transducers and the thermocouple reading indicate thermal equilibrium.

Air enclosures were modeled by means of EPS polystyrene square boards with a nominal thickness of 0.01 m and a side length of 0.3 m, in which a coaxial square hole with a side of 0.102 m was formed. The location and size of the hole correspond to the location and size of the planar heat flux transducer. These boards were inserted into the measuring space of the measuring device and thus formed vertical walls defining air enclosures of different heights with the maximum possible thickness of the vertical walls of the enclosure. Based on previously performed measurements and subsequent calculations by / ass. Prof. Sulc / and with the support of a qualified estimate of a worker of the manufacturer service organization, it can be assumed that the vertical walls of the enclosure can be considered as a re-emitting (or refractory) surface.

The experimental results were calculated by utilizing initially the Q-Lab software, which displays the readings of samples for over a certain time period until it reaches the equilibrium point, followed by Python program and Microsoft Excel for calculation of heat flux components.

As it was mentioned in the theoretical part, radiation is a complex phenomenon, and consideration of the wavelength and direction dependence of properties, assuming sufficient data exist, makes it even more complicated. Real surfaces do not emit radiation in a perfectly diffuse manner as a blackbody does. The variation of emissivity with direction for both electrical conductors and nonconductors is given in Fig. 9. Here θ is the angle measured from the normal of the surface, and thus $\theta = 0$ for radiation emitted perpendicularly to the surface. Note that ε_θ remains nearly constant for about $\theta < 40°$ for conductors such as metals and for $\theta < 70°$ for nonconductors such as plastics. Therefore, the directional emissivity of a surface in the normal direction is representative of the hemispherical emissivity of the surface [7].

For real surface: $\varepsilon_\theta \neq$ constant

$\quad\quad\quad\quad\quad \varepsilon_\lambda \neq$ constant

For diffuse surface: $\varepsilon_\theta =$ constant

For gray surface: $\varepsilon_\lambda =$ constant

For diffuse, gray surface: $\varepsilon = \varepsilon_\lambda = \varepsilon_\theta =$ constant
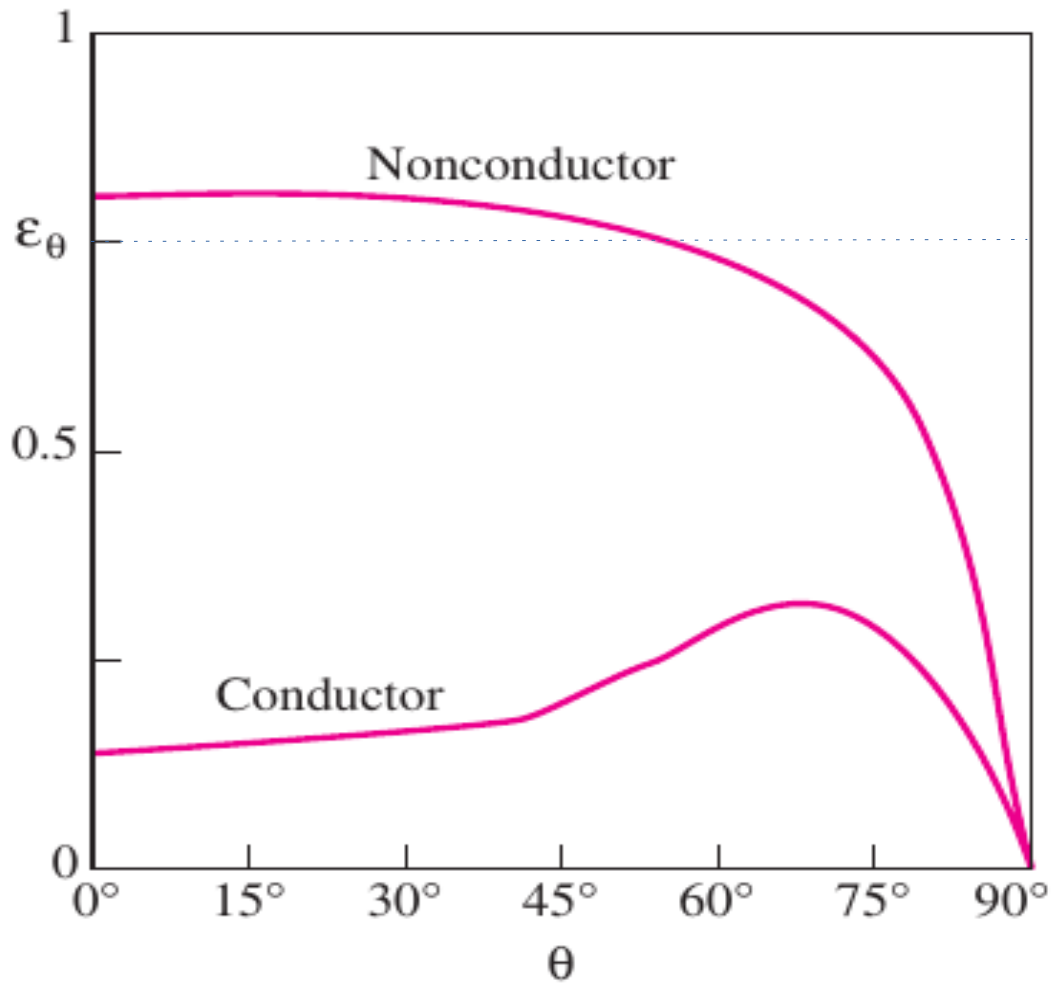
Figure 9: The variation of emissivity with direction for both electrical conductors and nonconductors [7][22].
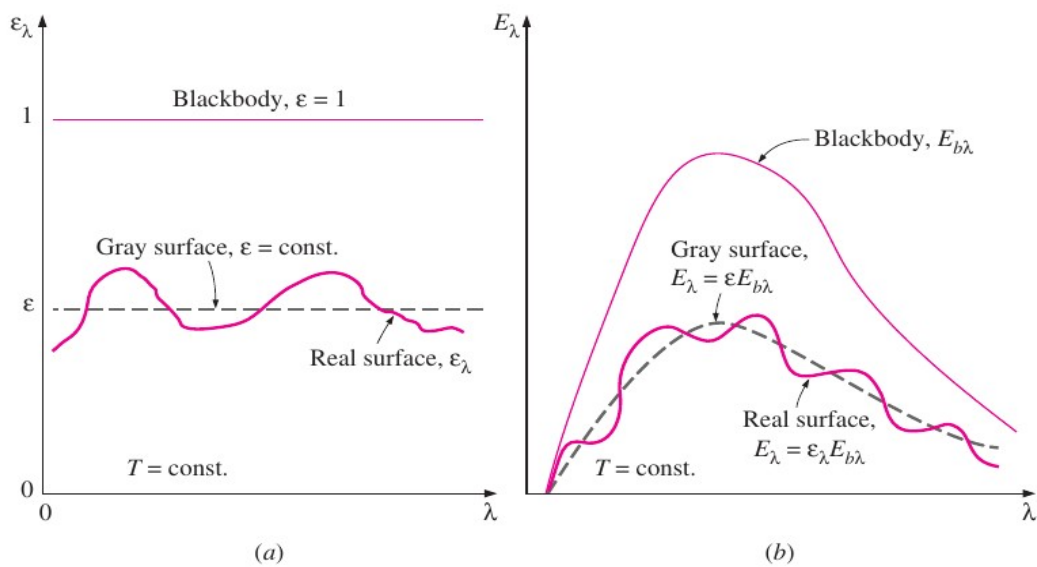

Figure 10: Comparison of the emissivity (a) and emissivity power (b) of a real surface with those of s gray surface and a blackbody at the same temperature [7].

The effect of the gray approximation on emissivity and emissive power of a real surface is illustrated in Fig. 10. Note that the emission of radiation from a real surface normally differs from the Planck distribution, and the emission curve may have multiple peaks and valleys. A gray surface should emit as much radiation as the real surface it represents at the same temperature.

Care should be exercised in the use and interpretation of radiation property data reported in the literature, since the properties strongly depend on the surface conditions such as oxidation, roughness, type of finish, and cleanliness. Consequently, there is considerable discrepancy and uncertainty in the reported values. The uncertainty here is mainly due to the difficulty in characterizing and describing the surface conditions accurately [7].

Dependencies presented in Fig. 9 are the total directional emissivities $\varepsilon_\theta(\theta,\varphi,T)$ defined as the ratio of the total intensity of radiation emitted by the surface at a specified direction to the total intensity of radiation emitted by an ideal blackbody at the same temperature.

$$\varepsilon_\theta(\theta,\varphi,T) = \frac{I_e(\theta,\varphi,T)}{I_b(T)}$$

(31)

These dependencies were obtained experimentally [7][21][13] by means of a relatively complicated measuring arrangement for a narrow, well collimated beam of thermal radiation.

The black coating, Nextel Velvet Black 811-21, was chosen as an example of a well-known coating with high and stable emissivity in the MIR (middle infrared).

The directional spectral emittance of gold and Nextel Velvet Black 811-21 sample measured at different polar angles as follows,
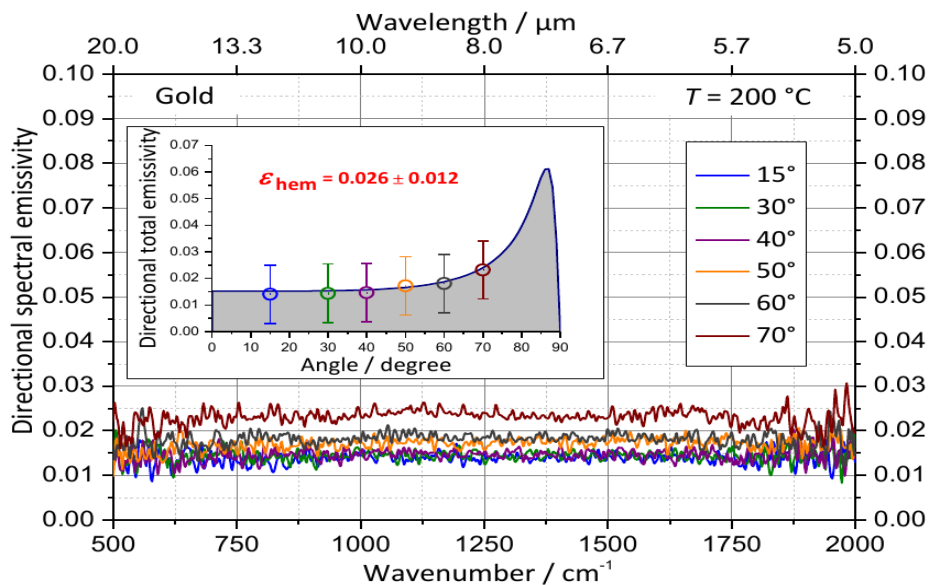

Figure 11: The directional spectral emittance of a gold sample measured at different polar angles [13].
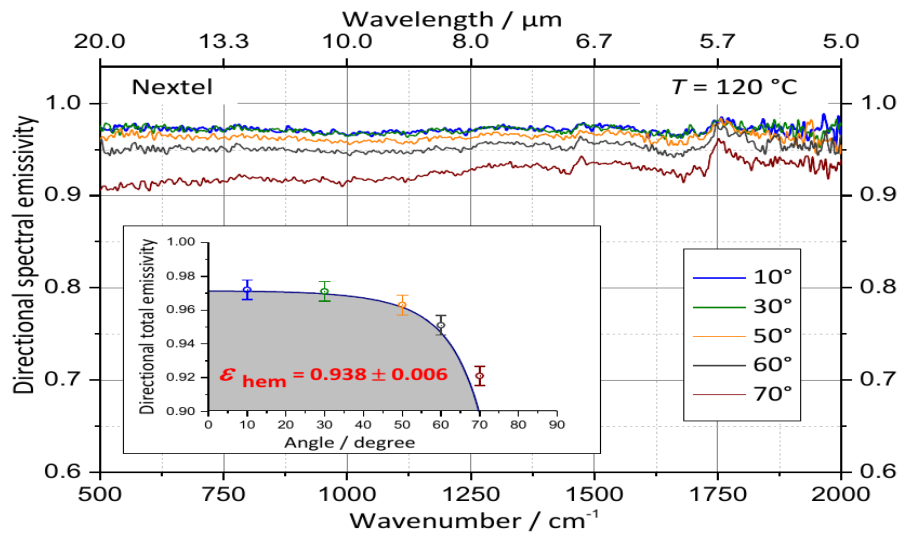
*Figure 12: Angular distribution of the directional spectral emittance of
Nextel Velvet Black 811-21 measured at a temperature of 120 °C [13].*

The total directional emittances of gold together with their standard uncertainties (circles with point) are shown in Fig. 11, with values from a fitted model (solid line) based on Fresnel equations. In contrast to materials with a relatively high emissivity (Nextel, or other dielectrics), the directional emissivity of metals remain low for smaller angles of observation and increases to a maximum for larger angles with a sharp decrease to zero for 90°[13].

With respect to variations of emissivity with direction for electrical conductors and nonconductors, three materials different in electrical conductivity were used as horizontal surfaces delimiting the modeled air enclosures. In the first series of measurements, these surfaces were directly the surface of the hot and cold plate of the measuring device, for their high value of surface electrical resistance (~ 2MΩ). In the second series, the horizontal surfaces were formed by a square-shaped aluminum foil (representing conductors) with a side of 0.2 m, oriented by a glossy surface inside the enclosure. In the third series, these surfaces were formed by a sheet of white A4 paper of the diplomat brand (representing nonconductors).

Note. In the following text, the term "assembly thickness" is used, which in the case of the first series of measurements is identical with the thickness of the air layer of the enclosure. In the case of the second and third series of measurements, the thickness of the assembly is greater than the thickness of the corresponding air layer by the thickness of two aluminum foils, respectively the thickness of two sheets of paper.

The experimental solution of the heat transfer in a horizontally oriented rectangular air enclosure is an easily solvable task in the arrangement described above. If both the upper and lower horizontal surfaces of the enclosure are isothermal and the temperature of the upper surface is higher than the temperature of the lower surface, the most important mechanisms of heat transfer in the enclosure are heat conduction in the air layer and heat transfer by radiation from the enclosure defining surfaces. Using the measured data, it is possible to determine the total heat flux through the enclosure and its conductive component. From their difference, the corresponding radiant component of the heat flux can be simply determined.

For the exact analytical expression of the radiant component of the heat flux through the enclosure, it would be necessary to take into account the spectral and angular emissivity distribution of the real horizontal surfaces delimiting the air enclosure. The vertical surfaces of the enclosure can be considered re-emitting, even though they are not an isothermal surface and the temperature of these surfaces takes on values between the temperature of the lower and upper horizontal surfaces of the enclosure.

Based on experimental results, it is not possible to draw any conclusions regarding the spectral dependence of the emissivity of the surfaces delimiting the modeled air enclosures.

Due to the significant change in the height of the air enclosure in each series of measurements, it is possible to draw some qualitative conclusions regarding the angular dependence of the emissivity of the horizontal surfaces of the enclosure. The maximum angle of emission ANM(I) of a photon directed from the upper surface of the enclosure to the lower surface of the enclosure decreases with increasing height of the enclosure. This angle is also the minimum angle of photon emission directed from the upper surface of the enclosure to the vertical surface of the enclosure. Its size decreases with increasing height of the enclosure.

At the end of the theoretical part the Eqn. (30) is presented for the calculation of radiant flux through a modeled air enclosure with diffusely emitting surfaces and re-emitting vertical surfaces of the enclosure. This equation contains expressions for space resistance for combinations of radiating surfaces 1 - 2, 1 - 3 and 3 - 2. Each of these expressions contains a corresponding view factor determined under the assumption of an even (diffuse) distribution of emission angles. However, this assumption does not apply in the whole range of possible emission angles $(0 \rightarrow \pi/2)$ of real surfaces as follows from the dependencies shown in above given Fig. 9.

An optimal solution to determine the radiant flux passing through the air enclosure, in this case, would be to determine the view factor for the horizontally oriented surfaces of the enclosure based on the real angular distribution of the photons emitted from the real surface.

When the surfaces are not diffuse – when emission or reflection varies with angle, some other methods of heat exchange representation can be applied. Among them, the Monte Carlo technique is probably the most widely used.

  In my diploma thesis, a simpler, less correct solution was chosen. This solution was directed to the determination of the "effective" emissivity value of three materials differing in the size of the electrical resistance and forming the horizontal surfaces of the air enclosure. The determination of the effective value of emissivity was always made for seven heights of the air layer of the enclosure. In this solution, the method of calculating view factors for parallel horizontal surfaces of the enclosure, based on the assumption of a diffusely emitting surface, was preserved. The experimentally determined thermal conductivity of the air enclosure VM (I) was compared with the calculated thermal conductivities of the enclosure VV (I,K) determined using Eqn. (30). These conductivities were calculated for monotonically increasing emissivities of the horizontal surfaces of the enclosure evenly distributed in the assumed emissivity interval of the material in the vicinity of the tabulated or otherwise defined emissivity of the material. If the experimentally determined thermal conductivity of the enclosure was between two immediately following values of the calculated thermal conductivities of the enclosure, the "effective" emissivity value of the horizontal surfaces for a given height of the air layer was determined by linear interpolation.

In each series, seven measurements were made for the gradually decreasing thickness of the air enclosure-forming assembly. The thickness of the assembly was determined using an LVDT sensor. All measurements were performed for the nominal mean temperature of the air layer t_n = 20 ºC and for the nominal temperature difference on the plates of the measuring device Δt_n = 20 K. When the equilibrium state was reached, the actual hot plate temperature – TU, the actual cold plate temperature – TL, actual mean temperature of the air layer –TM, the thermal resistance of the assembly – R, thickness of the assembly – ZS and thickness of the air layer – Z, were recorded.

Using these measured values, the following quantities were calculated for each air layer thickness:

QT (I) [W] - total heat flux through the assembly,

 QK (I) [W] – conductive component of the total heat flux through the air layer,

QR (I) [W] - radiant component of the total heat flux through the air layer,

VM (I) [W/(m^2.K)] - experimentally determined thermal conductivity of the air layer,
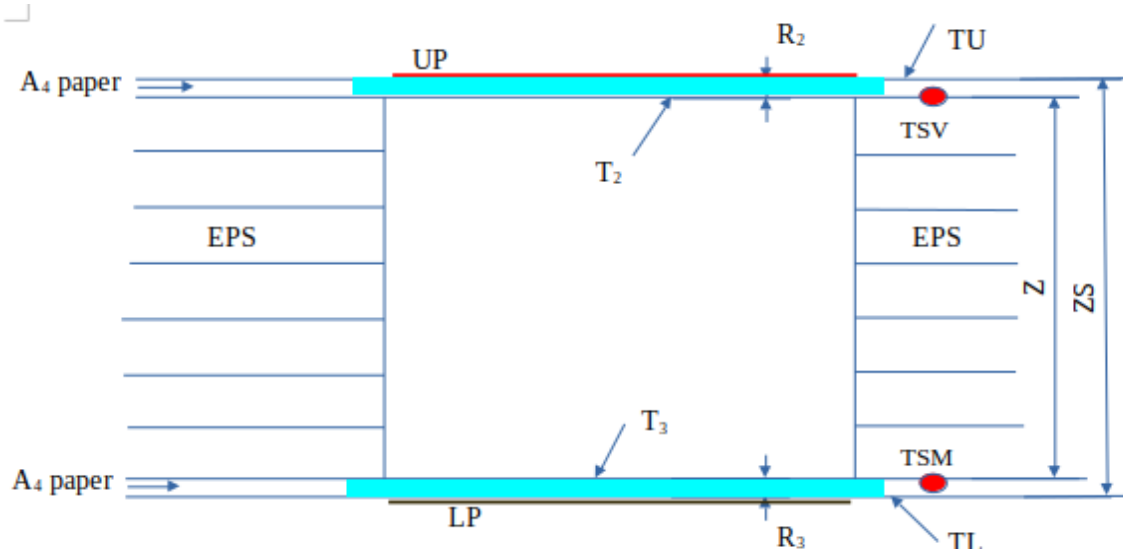
Figure 13: Schematic representation of experimental arrangement for sheet of paper measurement with important quantities [own].

FHH (I) - view factor for horizontal surfaces of the enclosure $1 - 2$ for given thickness of the air layer,

FHC (I) - view factor for surface 1 and 3 (from surface 1 to four vertical surfaces of the air enclosure), FHC(I) = 1.0 - FHH(I),

QSC (I,K) [W] - calculated radiant flux passing through a given thickness of the air layer, assuming that the vertical surfaces of the enclosure can be considered as a re-emitting surface. Index (K,K=1→7) expresses that QSC(I,K) values were calculated for seven evenly distributed emissivity value of the horizontal surfaces of enclosure,

ACL (I,K) – quantity with dimension [W/(m.K)] corresponding to QSC (I,K),

VV (I,K) - thermal conductivities calculated by means of QSC (I,K) quantities for given thickness of the air layer,

$$VV(I,K) = \frac{(ACL(I,K) + CL)}{Z(I)} \ , \tag{32}$$

CL [W/(m.K)] – experimentally determined coefficient of the thermal conductivity of air at 20 °C,

EIT (I) - effective value of emissivity of horizontal surfaces of the enclosure for a given thickness of the air layer. This emissivity value is determined on the basis of the experimentally determined thermal conductivity VM (I) of the air layer by linear interpolation between the values VV (I) and VV (I + 1) and their corresponding emissivity values E (K) and E (K + 1).

$$EIT(I) = E(K) + \frac{(VM(I) - VV(I,K))}{(VV(I,K+1) - VV(I,K))} \cdot ST \ , \tag{33}$$

ST – constant difference between emissivities E(K+1) and E(K), QSE (I) [W] - radiant flux passing through a given thickness of the air layer calculated according to Eqn. (30) for the effective value of emissivity EIT(I) of the horizontally oriented surfaces of the enclosure.

CHAPTER - 4

4.1 RESULT AND DISCUSSION

In the first series of measurements, the hot and cold plate were directly used as horizontal surfaces delimiting the air enclosure. The hemispherical emissivity of the plate surface, according to the statement of the responsible person of the measuring device manufacturer, would be in the range of 0.9 to 0.95. The QSC (I, K) values and corresponding VV (I, K) values were calculated for seven emissivities evenly distributed in the interval from 0.8 to 0.98 (with step 0.03). Using the Eqn. (30) (EIT(I)) the effective value of emissivity – EIT(I) was determined for all thicknesses of the air layer of the enclosure.

Table 6: Measured values for horizontally oriented surfaces represented by upper and lower plate of measuring instrument.

Test no.	ZS [m]	Z [m]	TU [°C]	TL [°C]	TM [°C]	R [m².K/W]
S1	0.011415	0.011415	29.45	9.49	19.47	0.155758
S2	0.022733	0.022733	30.23	9.8	20.02	0.192334
S3	0.033898	0.033898	30.4	9.72	20.06	0.213025
S4	0.045399	0.045399	30.5	9.68	20.09	0.230978
S5	0.057011	0.057011	30.56	9.59	20.07	0.249349
S6	0.068083	0.068083	29.92	9.7	19.81	0.268508
S7	0.079238	0.079238	29.95	9.65	19.8	0.284241

Table 7: Calculated values for horizontally oriented surfaces represented by upper and lower plate of measuring instrument.

Z [m]	QT [W]	QK [W]	QR [W]	VM [W/(m².K)]	EIT [-]	QSE [W]
0.011415	1.3332	0.42024	0.91301	6.4202	0.91375	0.91281
0.022733	1.1051	0.21599	0.88914	5.1993	0.92373	0.88905
0.033898	1.0100	0.14662	0.86338	4.69423	0.93675	0.86321
0.045399	0.93780	0.11022	0.82758	4.3294	0.94186	0.82748
0.057011	0.87497	0.088400	0.78657	4.0104	0.93594	0.78647
0.068083	0.78347	0.071386	0.71210	3.7243	0.92117	0.71208
0.079238	0.74304	0.061571	0.68146	3.5181	0.91035	0.68142

In the second series of measurements, the upper and lower horizontal surfaces of the enclosure were made of aluminum foil with a glossy surface oriented inside the enclosure.

The foil thickness $d_{Al}=21.48 \cdot 10^{-6}$ m was determined from the weight of a square of aluminum foil with a side of 0.1 m by using a mass density relationship.

$$m_{Al}=\rho_{Al}*d_{Al} \tag{34}$$

An aluminum has a density of 2.7 grams per cubic centimeter, ρ_{Al} = 2.7 g/cm^3 [17][22] and m_{al} = 5.8515 mg/cm^2. From this relationship the thickness of the aluminum foil is calculated as follow

$$d_{Al}=\frac{m_{Al}}{\rho_{Al}}=\frac{0.0057999\,g/cm^2}{2.7\,g/cm^3}=2.148111*10^{-2}\,mm \tag{35}$$

Temperature difference for the calculated thickness is determined as follow

$$QC=\frac{\lambda_{Al}*A}{d_{Al}}\Delta T \tag{36}$$

$$\Delta T=\frac{QC*d_{Al}}{\lambda_{Al}*A}=\frac{0.46794*21.48111*10^{-6}}{250*1.0404}=3.864*10^{-6}\,K$$

For the maximum value of the experimentally determined total heat flux QC (1) = 0.46794 W (for the minimum height of the air layer) the temperature drop on one foil is 3.864 * 10^{-6} K. Due to this negligible temperature drop the radiant heat fluxes QSC (I, K) were calculated for the temperatures of the upper and lower horizontal surface of the enclosure equal to the temperatures TU (I) and TL (I), respectively.

 According to the data in the literature [7][21] the total hemispherical emissivity of commercial aluminum sheet and aluminum foil is 0.09. Therefore, the QSC (I, K) values and corresponding VV (I, K) values were in this case, calculated for eight emissivities evenly distributed in the interval from 0.075 to 0.11 (step 0.005). Using the Eqn. (30) (EIT(I)) the effective value of emissivity – EIT(I) was determined for all thicknesses of the air layer of the enclosure.

Table 8: Measured values for measurement with aluminum foil.

Test no.	ZS [m]	Z [m]	TU [°C]	TL [°C]	TM [°C]	R [m². K/W]
S1	0.011264	0.011264	29.64	10.35	19.99	0.428889
S2	0.022311	0.022311	29.78	10.06	19.92	0.795501
S3	0.033971	0.033971	29.82	9.92	19.87	1.099643
S4	0.044862	0.044862	29.83	9.84	19.84	1.305725
S5	0.05637	0.05637	29.82	9.77	19.8	1.470049
S6	0.067965	0.067965	29.68	9.61	19.64	1.619204
S7	0.079261	0.079261	29.02	8.16	18.59	1.727007

Table 9: Calculated values for measurement with aluminum foil.

Z [m]	QT [W]	QK [W]	QR [W]	VM [W/(m².K)]	EIT [-]	QSE [W]
0.011264	0.46794	0.41158	0.05636	2.3316	0.094059	0.056358
0.022311	0.25791	0.21242	0.04549	1.2571	0.075244	0.045486
0.033971	0.18828	0.14079	0.04749	0.90939	0.078090	0.047492
0.044862	0.15928	0.10709	0.05219	0.76586	0.085525	0.052190
0.05637	0.14190	0.085483	0.056417	0.68025	0.092339	0.056416
0.067965	0.128956	0.070970	0.05799	0.61759	0.095198	0.057988
0.079261	0.12567	0.063251	0.062419	0.57904	0.099829	0.062416

In the third series of measurements, the upper and lower horizontal surface of the enclosure was formed by a single sheet of Diplomat paper. The temperature dependence of the thermal conductivity coefficient of this paper was determined by measuring a layer consisting of 85 sheets with a total thickness of 0.008954 m. The thickness of one sheet of paper is

$$d_p = 1.053 \cdot 10^{-4} \, m$$.

In the temperature range from 9.7 to 34.04 $°C$, this dependence was expressed with sufficient accuracy by linear fit.

Y = a + bx, where x = 0.06737 and y = 2.48702 * 10 $^{-4}$

$$\lambda_p = 0.06737 + 2.4087 \cdot 10^{-4} \cdot t \tag{37}$$

From this linear function, the coefficient thermal conductivity at 20 °C is (λ_{20} = 0.0721874

W/(m.K)). $$QC = \frac{\lambda_p * A}{d_p} \Delta T \tag{38}$$

$$\Delta T = \frac{QC * d_p}{\lambda_{20} * A} = \frac{1.1152 * 1.053 * 10^{-4}}{0.0721874 * 1.0404} = 0.16 \, K$$
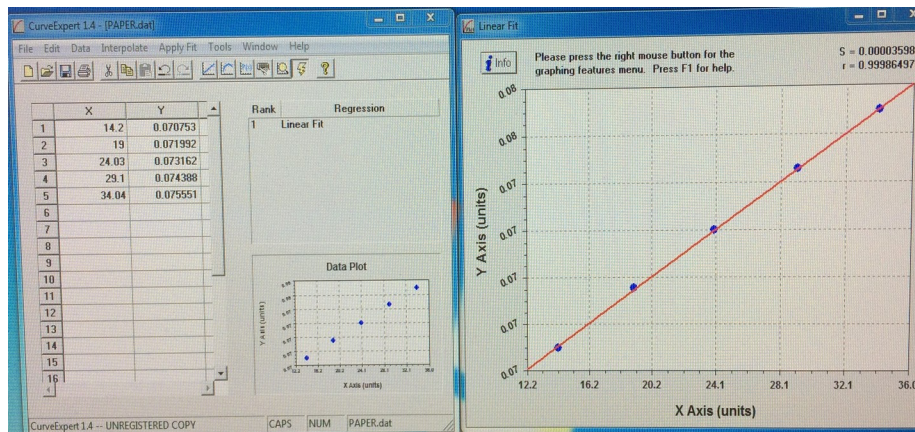

Figure 14 Linear function representing Temperature dependence of coefficient of thermal conductivity of paper by using Curve Expert program [own].

For the maximum value of the experimentally determined total heat flux QC (1) = 1.1152 W (for the minimum height of the air layer), the maximum temperature drop on one sheet of paper was 0.16 K. In this series of measurements, the corresponding temperature drop was taken into account by temperatures T2 (I) and T3 (I), the actual temperatures of the upper and lower surface of the enclosure. Radiant heat fluxes QSC (I, K) were calculated for these temperatures.

According to the data in the literature [7][21] the total hemispherical emissivity of white paper is 0.09. Therefore, the QSC (I, K) values and corresponding VV (I, K) values were calculated for eight emissivities evenly distributed in the interval from 0.075 to 0.11 (step 0.005). Using the Eqn. (30) (EIT(I)) the effective value of emissivity – EIT(I) was determined for all thicknesses of the air layer of the enclosure.

Table 10: Measured values for measurement with sheet of Diplomat paper.

Test no.	ZS [m]	Z [m]	TU [°C]	TL [°C]	TM [°C]	R [m². K/W]
S1	0.011481	0.011270	30.08	10.29	20.19	0.184718
S2	0.022813	0.022602	29.63	10.29	19.96	0.223345
S3	0.033962	0.033751	29.67	10.16	19.91	0.243929
S4	0.04544	0.045229	29.7	10.08	19.89	0.262092
S5	0.057083	0.056872	29.71	10.01	19.86	0.279049
S6	0.068201	0.067990	29.61	9.83	19.72	0.292651
S7	0.079355	0.079144	30.48	9.7	20.09	0.314452

Table 11: Calculated values for measurement with sheet of Diplomat paper.

Z [m]	QT [W]	QK [W]	QR [W]	VM [W/(m².K)]	EIT [-]	QSE [W]
0.011270	1.1152	0.41555	0.69966	5.5006	0.78220	0.69966
0.022602	0.90091	0.20295	0.69795	4.5367	0.82463	0.69787
0.033751	0.83214	0.13726	0.69488	4.1492	0.84776	0.69476
0.045229	0.77884	0.10309	0.67574	3.8585	0.85744	0.67572
0.056872	0.73449	0.082377	0.65211	3.6215	0.85986	0.65212
0.067990	0.70320	0.069220	0.63398	3.4515	0.86280	0.63396
0.079144	0.68753	0.062515	0.62501	3.2099	0.83667	0.62498

The dependence of the ANM on the height of the air layer for first series of measurement is demonstrated as follows

Table 12: The relationship between the height of the air layer and corresponding maximum angle ANM(I) for the first series of measurement.

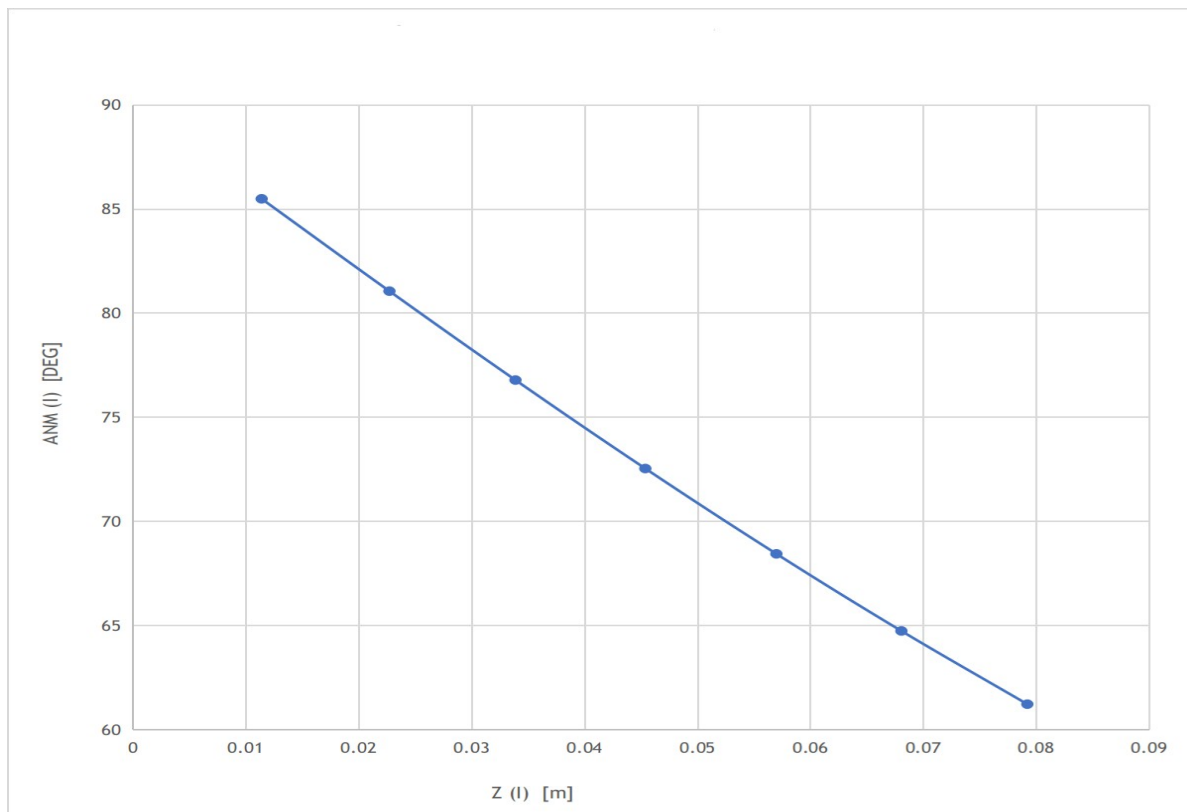| Sample no. (I)	Z(I) [m]	ANM(I) [RAD]	ANM(I) [DEG]
1	0.011415	1.4918	85.475
2	0.022733	1.4145	81.044
3	0.033898	1.3400	76.776
4	0.045399	1.2659	72.530
5	0.057011	1.1944	68.435
6	0.068083	1.1298	64.734
7	0.079238	1.0685	61.220

Figure 15: The dependence of the ANM (I) on the height of the air layer for the first series of measurement.

From Fig. 15 shows the values of maximum angles for the first series of measurement. It can be observe that there is a gradually decrease in ANM from around 85 to 60 degree with increasing of the height of the air layer, Z.

For the second (measurement with aluminum foil) and third (measurement with sheet of Diplomat paper) series of measurement values are quite similar to the first series of measurement. The difference is observed only after two decimal digit.

Here the demonstration of the dependence of effective emissivity (EIT) on the height of the air layer for the all three series of measurements.
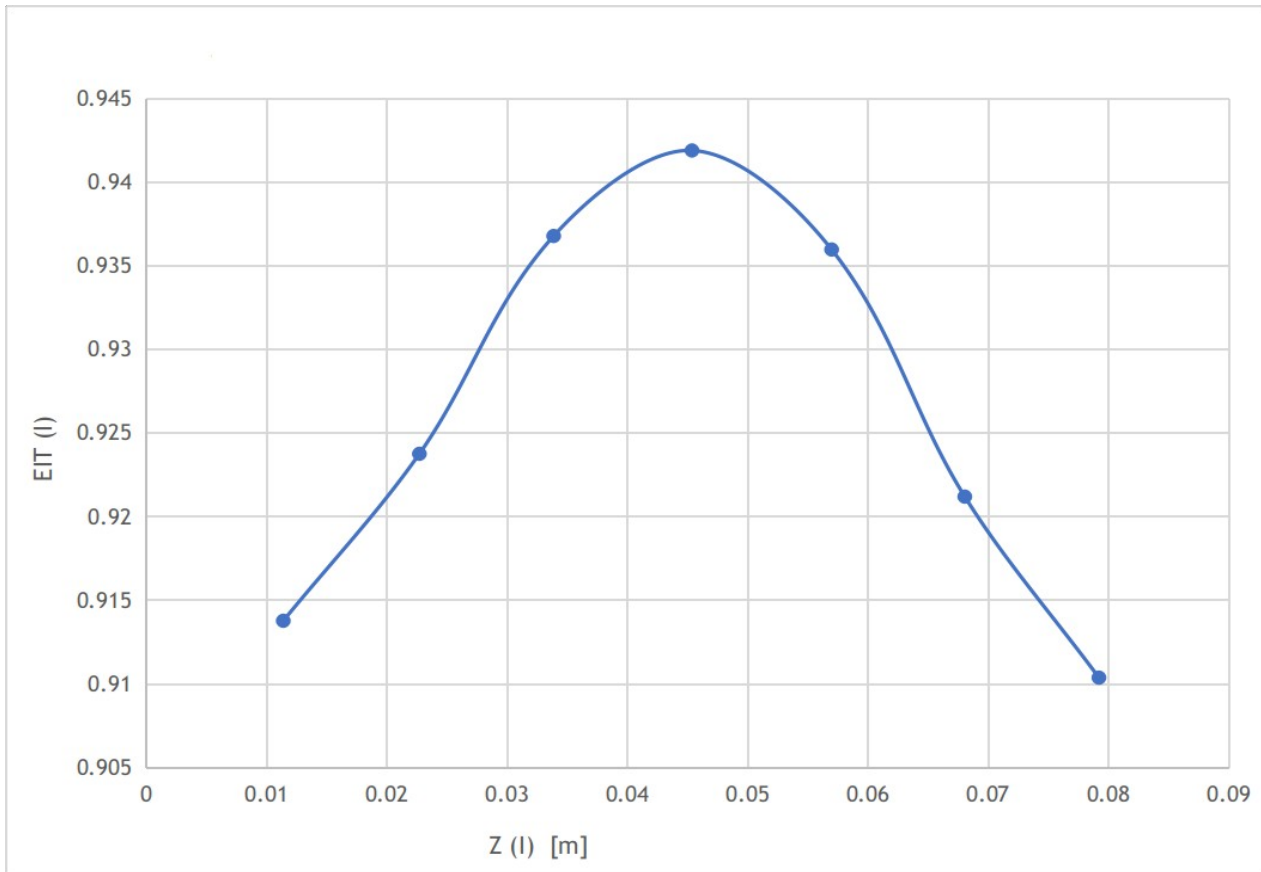

Figure 16: The dependence of the EIT on the height of the air layer for the first series of measurement.

Fig. 16 shows the values of EIT for the measurement carried out with upper and lower plate of measuring instrument directly delimiting horizontally oriented surfaces of air enclosure, not including the additional materials used in following measurements (first series of measurement). It can be obeseve that there is a gradually increase in EIT till a maximum value of 0.94186 at the height of the air layer, Z = 0.0454 m. Following this a gradual decrease in EIT it can be observed till maximum Z = 0.07924 m.
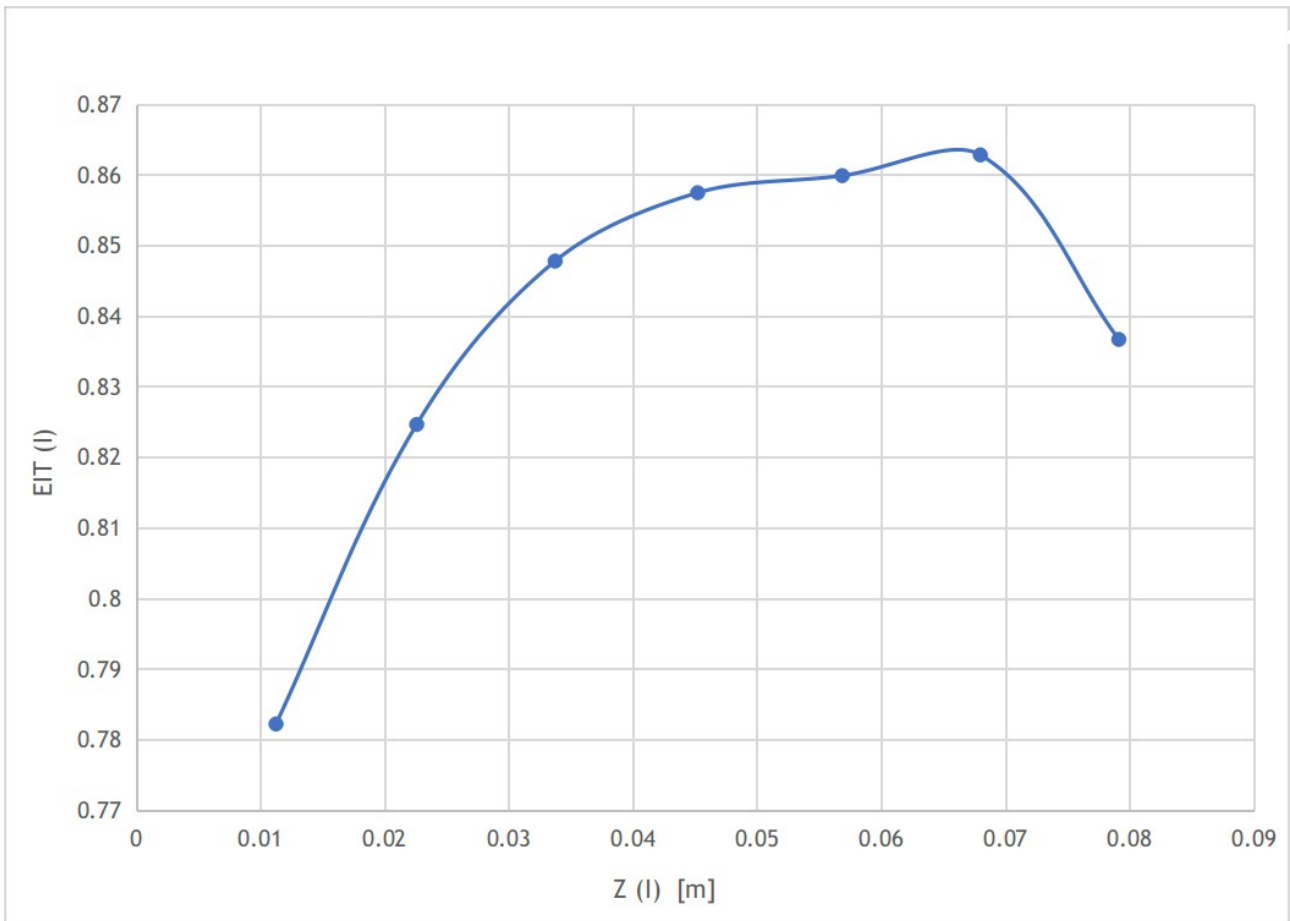
Figure 17: The dependence of the EIT on the height of the air layer for the third series of measurement.

Fig. 17 shows the values of EIT for the measurement carried out with aluminum foil (second series of measurement). It can be obeseve that initially there is a gradually decrease in EIT till $Z = 0.0226$ m and then for the rest of the height of the air layer, a gradually increment of EIT is observed. A maximum value of EIT = 0.0998 at the the height of the air layer, $Z = 0.07926$ m is recorded.
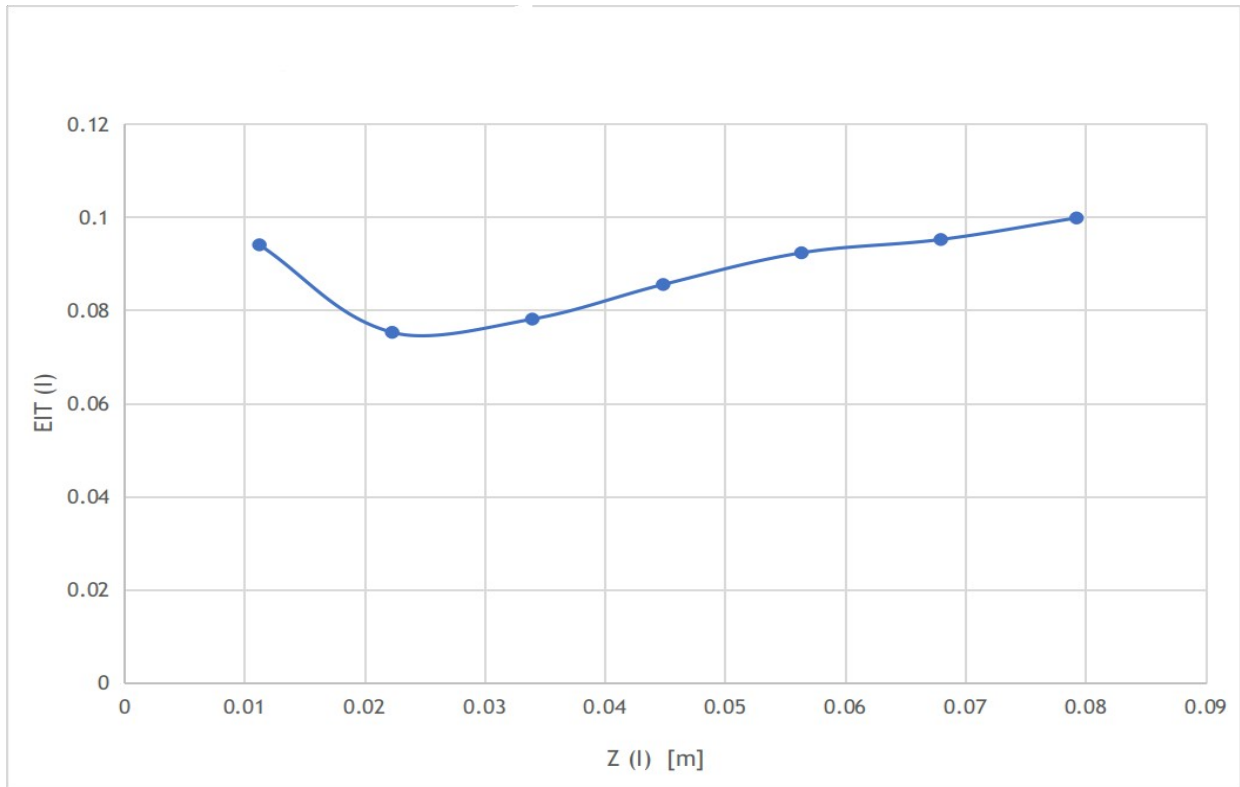
Figure 18: The dependence of the EIT on the height of the air layer for the second series of measurement.

Fig. 18 shows the values of EIT for the measurement carried out with A4 paper of the diplomat brand (third series of measurement). It can be obeseve that there is a gradually increase in EIT till a maximum value of 0.8628 at the the height of the air layer, $Z = 0.06799$ m. Following this a gradual decrease in EIT it can be observed till maximum $Z = 0.07914$ m .

CHAPTER - 5

5.1 CONCLUSION AND RECOMMENDATION

In Figs. 16 to 18, the dependence of the effective emissivity of the horizontal surfaces of the enclosure on the height of the enclosure is demonstrated.

In Tab. 12 the relationship between the height of the enclosure and its corresponding maximum angle ANM(I) [deg] is shown for the third series of measurement (there are differences on the second decimal place of ANM(I) for other series of measurements).

For any of the materials forming the horizontal surfaces of the air enclosure, I did not find in the professional literature the dependence of their total directional emissivity on the emission angle, as it is shown in Fig. 9 for two groups of materials.

For uneven distribution of emission angles from real surfaces, it is not possible to use the relations reported in the literature for the calculation of view factors, because radiation exchange between diffuse surfaces only is assumed.

Therefore, the view factor FHH (I) for each height of the air layer was calculated as for the diffusely emitting surface. In such a case it was also possible to determine the magnitude of the spatial resistances in the equation for calculation of the radiant flux through the air enclosure with re-emitting vertical walls. In the manner already described above, the effective emissivities EIT (I) of the horizontal surfaces of the enclosure were determined using the experimentally determined thermal conductivity of the enclosure VM (I) and the calculated thermal conductivities of the enclosure VV (I, K).

The effective emissivity determined in this way should be considered as the mean value of emissivity for a wide range of emission angles from 0 to ANM (I), including the influence of directional and spectral emissivity distribution of real surfaces. The fact that the magnitude of the view factors FHH (I) were not determined for unevenly distributed emission angles from the real surface is transferred into the magnitude of the EIT (I).

From the dependencies shown in Fig. 9 and taking into account the sizes of ANM (I) in Tab. 12, it is clear that in the stated range of maximum emission angles AMN (I), the magnitude of the total directional emissivity changes most significantly for both groups of compared materials. It can be assumed that the EIT (I) values for small air enclosure heights and thus large ANM (I) angles may be more affected.

An accurate determination of the effective emissivity of the horizontal surfaces of the enclosure, which would be in accordance with the results obtained experimentally, is not possible without knowing the angular dependence of the total directional emissivity of the real surface.

It is recommended that based on experimental results, verifying the possibility of determining the effective emissivity of horizontal surfaces of the air enclosure if these surfaces are formed by a thick layer of electrically conductive and non-conductive materials.

REFERENCE

[1] M. Jilek, Thermomechanics. CVUT Praha, 2000.

[2] P. Urone and R. Hinrichs, "College Physics - OpenStax," 2021. https://openstax.org/details/books/college-physics (accessed May 17, 2021).

[3] J. Lienhard IV and J. Lienhard V, A Heat Transfer Textbook, 3rd edition. Phlogiston Press, 2008.

[4] A. V. Vidyapeetham, "Heat transfer by Conduction (Theory) : Heat & Thermodynamics Virtual Lab : Physical Sciences : ," 2011.

[5] Autodesk, "Isotropic Material Properties (Thermal)." https://download.autodesk.com/us/algor/userguides/mergedprojects/setting_up_the_analysis/thermal/Materials/Isotropic_Material_Properties.htm#:~:text=Thermal conductivity %3A,applicable to all thermal elements (accessed Jun. 02, 2021).

[6] G. Ananthasayanan, "Heat transfer in horizontally oriented air enclosure," Technical University of Liberec, Liberec, 2020.

[7] Y. Cengel, Heat and mass transfer : a practical approach, 3rd edition. Boston, Mass. : McGraw-Hill, 2014.

[8] Admin, "Natural convection: Natural convection inside enclosures | hydraulics and pneumatics," 2016. http://machineryequipmentonline.com/hydraulics-and-pneumatics/natural-convectionnatural-convection-inside-enclosures/ (accessed May 15, 2021).

[9] X. Zhang, "Demonstration of a new transport regime of photon in two-dimensional photonic crystal," Phys. Lett. Sect. A Gen. At. Solid State Phys., vol. 372, no. 19, pp. 3512–3516, May 2008, doi: 10.1016/j.physleta.2008.02.033.

[10] S. V. P. C. Arendra, "Spectral black body emissive power (Planck's law) Calculator | Calculate Spectral black body emissive power (Planck's law)." https://www.calculatoratoz.com/en/spectral-black-body-emissive-power-(plancks-law)-calculator/Calc-15098 (accessed Jun. 04, 2021).

[11] M. A. H. Mamun, "Radiation lecture 1 nov 2013," 2013.

[12] S. Gupta, Unit-11 Theory of Radiation. Indira Gandhi National Open University, New Delhi, 2020.

[13] A. Adibekyan, "High-accuracy Spectral Emissivity Measurement for Industrial and Remote Sensing Applications," Bergische Universitat Wuppertal, Wuppertal, 2016.

[14] N. Wang, H. Shen, and R. Zhu, "Constraint optimization algorithm for spectral emissivity calculation in multispectral thermometry," Meas. J. Int. Meas. Confed., vol. 170, p. 108725, Jan. 2021, doi: 10.1016/j.measurement.2020.108725.

[15]   I. A. Wassan, "Heat Transfer-Fundamentals of thermal radiations," 2016.

[16]   Admin, "Radiation Heat Transfer: View factor | hydraulics and pneumatics," 2016. http://machineryequipmentonline.com/hydraulics-and-pneumatics/radiation-heat-transferview-factor-relations/ (accessed May 07, 2021).

[17]   W. G. Kannuluik and E. H. Carman, "The temperature dependence of the thermal conductivity of air," Aust. J. Chem., vol. 4, no. 3, pp. 305–314, 1951, doi: 10.1071/CH9510305.

[18]   Engineering ToolBox, "Emissivity Coefficient Materials," 2003. https://www.engineeringtoolbox.com/emissivity-coefficients-d_447.html?fbclid=IwAR3-X4eYCRv5E3AJRJG4LaW3WzTQp1bBWue11WMCaPlZ69ETD2NX8GgEvNs (accessed Jun. 01, 2021).

[19]   Infrared-thermography, "Emissivity Values for Common Materials." https://www.infrared-thermography.com/material.htm (accessed May 10, 2021).

[20]   Engineering ToolBox, "Thermal Conductivity of some selected Materials and Gases," 2003. https://www.engineeringtoolbox.com/thermal-conductivity-d_429.html?fbclid=IwAR0Es75fgQETTM7le3MGiJq_ZODBfjqr6moaVHZT-t8A4gnGmo8rBmUoA8U (accessed Jun. 06, 2021).

[21]   Neutrium, "Calculation of Emissivity for Metals | Neutrium," 2018. https://neutrium.net/heat-transfer/calculation-of-emissivity-for-metals/ (accessed April 04, 2021).

[22]   Usetute, "Density Calculations Chemistry Tutorial." https://www.ausetute.com.au/density.html?fbclid=IwAR0ePuRWO2Yo1hd3GwU2vD3hC7--N8-fz97oSYGhfztxjSMx9gr_JBAYdW0 (accessed Jun. 02, 2021).

[23]   Netzsch Co., "HFM 446 Lambda Series-Heat Flow Meter for Testing Insulation Materials." .